INVESTIGATION OF THE ATMOSPHERIC CHEMISTRY OF BROMINE-CONTAINING COMPOUNDS

Report to the
Brominated Solvents Consortium
Contract CF9901151218

by

William P. L. Carter and Ernesto C. Tuazon

September 27, 2000

Air Pollution Research Center
University of California
Riverside, California 92521

ABSTRACT

Experiments were carried out to investigate the gas-phase reactions of simple bromine compounds under atmospheric conditions to provide data aimed at reducing uncertainties in model calculations of the atmospheric ozone impacts of propyl bromide and other bromine containing compounds. The reactions of HBr with O_3, HBr with O_3 and formaldehyde with NO or NO_2 in the dark and upon irradiation, and the irradiations of Br_2 in the presence of formaldehyde and/or NO_x were studied. The experiments were carried out in air at atmospheric pressure and ambient temperature in a 5870 liter evacuable Teflon-coated chamber with quartz end windows and a xenon arc solar simulator light source. In-situ FT-IR spectroscopy was used to monitor most reactants and products. Most experiments used dry air, except for the HBr + O_3 runs with varying humidity.

Ozone was found to react with HBr with an apparent rate constant of 4×10^{-19} cm^3 $molec^{-1}$ s^{-1}, with the data suggesting that HOBr is formed in the initial reaction, but that it reacts with HBr to form Br_2, with a rate constant of at least 3.5×10^{-15} cm^3 $molec^{-1}$ s^{-1}. Humidity affected the HBr wall loss rate but did not affect the apparent O_3 + HBr rate constant, suggesting that the reaction of HBr with O_3 may not be surface dependent. In the presence of NO_x the reactions of Br_2 or HBr caused consumption or transformations of NO and NO_2 and formation of varying amounts of BrNO and $BrNO_2$. Attempts to model the experiments in the presence of NO_x were unsuccessful. The data obtained indicated that the mechanism used in the previous study of Carter et al (1997) to account for the observed ozone reactivity of propyl bromide was incorrect, and no mechanism was found that is consistent with the data. The data are also ambiguous concerning the role of wall effects in this system. It is concluded that considerable fundamental research is required on the reactions of bromine containing species in the presence of NO_x before we can predictively model the atmospheric reactions of bromine containing organics.

ACKNOWLEDGEMENTS

The authors thank Roger Atkinson for many helpful comments, and for providing partial funding for the experiments carried out in this project. We also acknowledge Sara M. Aschmann for assistance in carrying out the experiments.

This work was funded primarily by the Brominated Solvents Consortium, whose members are Albemarle Corporation, Dead Sea Bromine Group and Great Lakes Chemical Corporation. Additional funding was provided by the Air Pollution Research Center of the University of California at Riverside. However, the opinions and conclusions in this report are entirely those of the authors. Mention of trade names and commercial products does not constitute endorsement or recommendation for use.

TABLE OF CONTENTS

LIST OF TABLES

LIST OF FIGURES

INTRODUCTION

Many different types of volatile organic compounds (VOCs) are emitted into the atmosphere, each reacting at different rates and having different mechanisms for their reactions. Because of this, VOCs can differ significantly in their effects on ozone formation. The effect of a VOC on ozone formation is also referred to as its "reactivity." Some compounds, such as CFCs, do not react in the lower atmosphere at all, and thus make no contribution to ground-level ozone formation. Others, such as methane, react and contribute to ozone formation, but react so slowly that their practical effect on ozone formation is negligible. Since it does not make sense to regulate negligibly reactive compounds as ozone precursors, the EPA has exempted certain compounds from regulation in recognition of this. Although the EPA has no formal policy on what constitutes "negligible" reactivity, it has the informal policy of using the ozone formation potential of ethane as the standard in this regard (Dimitriades, 1999). Therefore, the ozone formation potential of a compound relative to ethane is of particular interest when assessing whether it might be a likely candidate for exemption from regulation as an ozone precursor.

1-Bromopropane (1-BP) is a low-reactivity compound that is of interest as an alternative solvent. Because of this, Albemarle, a producer of 1-BP, previously contracted the College of Engineering Center for Environmental Research and Technology (CE-CERT) at the University of California at Riverside (UCR) to investigate whether 1-BP and 1-bromobutane might be potential candidates from exemption from VOC regulations on the basis of low ozone reactivity (Carter et al, 1997). This study involved (1) conducting environmental chamber experiments to measure the effects of these compounds on ozone formation and other manifestations of photochemical smog when added to various model photochemical smog systems, (2) developing atmospheric reaction mechanisms for these compounds and evaluating these mechanisms by comparing their predictions against the results of the chamber experiments, and (3) using the mechanisms to predict the ozone impacts of the compounds under various atmospheric conditions. The results indicated that although these compounds can be expected to have low or negative ozone impacts under low NOx conditions, the magnitudes of these impacts, and their impacts under the higher NOx conditions which are most sensitive to VOC emissions, are highly uncertain. In the case of 1-BP, the range of uncertainty for the maximum reactivity is between approximately one and three times the reactivity of ethane, on an ozone formed per gram emitted basis (Carter et al, 1997). Because of this uncertainty, it may be difficult for the EPA to grant 1-BP an exemption on the basis of low reactivity relative to ethane.

The uncertainty in the ozone impact predictions for 1-BP was due to the fact that no chemically reasonable mechanism could adequately simulate the results of the environmental chamber experiments with that compound unless some unverifiable assumptions were made. In particular, it had to be assumed that there is a rapid reaction between O_3 and HBr, forming HOBr, which photolyzes rapidly to form OH + Br. However, preliminary experiments, carried out to investigate this possibility at the Air Pollution

Research Center (APRC) at UCR, indicated that this reaction is relatively slow, at least in the dark under ultra-dry conditions. This indicates that there must be some other process which is occurring in our chamber experiments which has the same effect as a rapid O_3 + HBr reaction, but whose exact nature is unknown. In particular, it is unknown whether this is a chamber effect which is not important in the atmosphere, or whether it represents some unknown aspect of atmospheric BrOx/HBr chemistry which needs to be added to atmospheric simulation models when predicting impacts of 1-BP and other bromine-containing species.

It was clear that additional studies are needed before definitive conclusions can be made concerning the atmospheric impacts of 1-BP and other bromine-containing compounds. At a minimum, it had to be determined whether there is indeed a reaction between O_3 and HBr (which may occur in the light or the presence of humidity or NO_x), and if so whether it is surface-dependent. In addition, systematic studies of ozone reactivities of simpler molecules, such as Br_2, HBr, and methyl bromide, would need to be carried out to elucidate what is occurring in chemically simpler systems. Only when we have confidence we understand these chemically simpler systems can we have a reasonable chance of understanding, and predictively modeling, ozone impacts for other bromine-containing organics such as 1-BP.

In view of this, Albemarle Corporation, on behalf of the Brominated Solvents Consortium, contracted APRC to carry out the additional studies on the simpler chemical systems involving bromine species that hopefully would elucidate these issues. The results of these experiments, and their implications concerning our understanding and ability to predictively model the atmospheric reactions of simple bromine-containing species and propyl bromide, are discussed in this report.

EXPERIMENTAL AND MODELING METHODS

Experimental Methods

Experimental Procedures

The experiments were carried out at 298 ± 2 K and 740 Torr total pressure of air in the Air Pollution Research Center's (APRC) 5870 L evacuable, Teflon-coated chamber, which is equipped with an in situ multiple-reflection optical system interfaced to a Nicolet 7199 Fourier transform infrared (FT-IR) absorption spectrometer. A solar simulator with a 24 kW xenon arc lamp provided the photolysis radiation which was filtered through a 0.25 in. thick Pyrex pane to remove wavelengths <300 nm.

Dry synthetic air (<10 ppm H_2O), a 20% O_2 (ultra-high purity, Puritan Bennett) and 80% N_2 (head gas from liquid N_2, BOC Gases) mixture, was the diluent gas for the majority of the experiments. For the few experiments which required higher humidities of up to 25% RH, weighed amounts of distilled H_2O (Optima grade, Fisher Scientific) were introduced into the evacuated chamber, which was then filled with air. Partial pressures of the reactants were measured into calibrated 2 L and 5 L Pyrex bulbs and injected into the chamber by flushing with a stream of N_2 gas.

FT-IR spectra were recorded with 64 scans (corresponding to 2-min averaging time) per spectrum, a full-width-at-half-maximum resolution of 0.7 cm^{-1}, and a path length of 62.9 cm^{-1}. Depending upon the particular reaction, either of two liquid N_2-cooled detectors was employed, an InSb (~1700-3800 cm^{-1}) detector for its higher sensitivity or an HgCdTe detector (~650-3200 cm^{-1}) for its wider spectral range. The spectra of the reaction mixture were analyzed by interactive subtraction of reference spectra of the reactants and known products, whereby the concentration of an analyte was expressed as a factor of the analyte content of the reference spectrum. The set of reference spectra were from authentic samples, such as those recorded for the organic products (e.g., acetone and ethyl formate) as well as those from the initial injections of the reactants (except for Br_2, whose fundamental vibrational mode is not active). The analyses also employed APRC's standing collection of calibrated reference spectra, recorded with the same spectral parameters as those of the present experiments, for species such as HONO, $HONO_2$, $HOONO_2$, N_2O_5, HCOOH, CO and CO_2.

For the quantitative analyses of the observed reaction products BrNO and $BrNO_2$, absorption coefficients derived from literature data were employed: for the BrNO P-branch at 1792 cm^{-1}, 8.6 x 10^{-3} ppm^{-1} m^{-1} (Broeske and Zabel, 1998); for the $BrNO_2$ R-branch at 1301 cm^{-1}, 5.4 x 10^{-3} ppm^{-1} m^{-1} (Frenzel et al., 1996).

Chemicals

HBr (99+%), Br_2 (99.99 +%), diethyl ether (99.9%), cyclohexane (99.9+%), and 2,3-dimethylbutane (98%) were from Aldrich. NO (99.0%) and NO_2 (99.5%) were from Matheson. Samples of HBr from the lecture bottle were pre-distilled through a trap at dry ice-acetone temperature and collected at liquid N_2 temperature prior to use. Gaseous HCHO was obtained from a degassed liquid/solid sample which was freshly distilled from paraformaldehyde (purified, Fisher Scientific Co.). O_3 in O_2 diluent was prepared as needed by passing O_2 (ultra-high purity, Puritan Bennett) through a Welsbach T-408 ozone generator at pre-calibrated flow and voltage settings.

Modeling Methods

Gas-Phase Mechanism

The gas-phase chemical mechanism used in all the model calculations discussed in this report is the "SAPRC-99" mechanism that is documented in detail by Carter (2000), with bromine reactions added as discussed in this report. All the VOCs used in experiments modeled in this report were represented explicitly using the individual VOC mechanisms given by Carter (2000), with reactions of Br added as appropriate.

The reactions added to the mechanism to represent bromine chemistry are given in Table 1, with footnotes documenting the reactions given in Table 2 and absorption cross sections and quantum yields used when calculating photolysis rates of bromine-containing species given in Table 3. These reactions were completely updated compared to the bromine mechanism used in the previous study of Carter et al (1997), based on a more comprehensive evaluation of literature data and on the results of the experiments carried out for this project, as discussed in the "Results" section. Explicit representations of species such as BrNO, $BrNO_2$, BrONO were added so the measurements of these species could be modeled where applicable, and a number of reactions involving these and other bromine-containing NO_x species were significantly modified as a result of this analysis. The most important reactions are discussed below in conjunction with discussion of the modeling of the experiments carried out for this program.

Environmental Chamber Simulations

The ability of the mechanism to represent the reactions occurring in this system was evaluated by modeling the experiments carried out for this program, and comparing the model predictions with the experimental data obtained. When modeling such experiments, it is necessary to include an appropriate representation of the spectrum and intensity of the light source and of the various chamber wall effects (Carter et al, 1995). The intensity was determined by carrying out NO_2 actinometry experiments as discussed in the following section. The Pyrex-filtered EC solar simulator spectrum used when modeling

Table 1. Reactions added to the base SAPRC-99 mechanism to represent the reactions of bromine-containing compounds.

Label	Rate Parameters [a]				Refs & Notes [b]	Reaction and Products [c]
	k(298)	A	Ea	B		
Inorganic BrO_x - HO_x - NO_x Reactions						
(1)	4.10e-19	4.10e-19			1	O3 + HBR = HOBR + O2
(2)	3.41e-15	3.41e-15			2	HOBR + HBR = BR2 + H2O
(9)	1.11e-11	1.10e-11	0.00	-0.8	3	HO. + HBR = H2O + BR.
BR04		(Slow)			4	NO3 + HBR = HNO3 + BR.
BR06		(Slow)			5	HO2. + HBR = HO2H + BR.
(8)	4.59e-11	1.20e-11	-0.79		3	HO. + BR2 = HOBR + BR.
BR07	3.78e-14	5.80e-12	2.98		6	O3P + HBR = HO. + BR.
BR08		Phot Set= HOBR			7	HOBR + HV = HO. + BR.
BR09		Phot Set= BR2			8	BR2 + HV = #2 BR.
BR10	8.98e-33	8.98e-33			9	BR. + BR. + M = BR2 + M
(4)	1.16e-12	1.70e-11	1.59		3	BR. + O3 = BRO. + O2
BR12	1.93e-12	1.40e-11	1.17		3	BR. + HO2. = HBR + O2
(10)	8.00e-32	8.00e-32			10	BR. + NO + M = BRNO + M
(11)	4.53e-12	Falloff, F=0.55			3,11	BR. + NO2 = BRONO
	0:	4.20e-31	0.00	-2.4		
	inf:	2.70e-11	0.00	0.0		
BR15	1.60e-11	1.60e-11			3	BR. + NO3 = BRO. + NO2
BR16	4.00e-12	4.00e-12			12	BR. + BRNO = BR2 + NO
BR17	4.00e-12	4.00e-12			12	BR. + BRNO2 = BR2 + NO2
BR18	5.80e-11	5.80e-11			13	BR. + BRONO2 = BR2 + NO3
(5)	2.11e-12	4.00e-12	0.38		3	BRO. + BRO. = #2 BR. + O2
(6)	3.85e-13	4.20e-14	-1.31		3	BRO. + BRO. = BR2 + O2
BR21		Phot Set= BRO			14	BRO. + HV = BR. + O3P
BR22		(Slow)			3	BRO. + O3 = BR. + #2 O2
(7)	6.20e-15	6.20e-15			15	BRO. + HBR = BR2 + HO.
BR24	3.32e-11	6.20e-12	-0.99		3	BRO. + HO2. = HOBR + O2
BR25	2.08e-11	8.70e-12	-0.52		3	BRO. + NO = BR. + NO2
BR26	2.86e-12	Falloff, F=0.40			3	BRO. + NO2 = BRONO2
	0:	4.70e-31	0.00	-3.1		
	inf:	1.70e-11	0.00	-0.6		
BR27	1.00e-12	1.00e-12			3,16	BRO. + NO3 = BR. + O2 + NO2
(13)		Phot Set= BRNO			17	BRNO + HV = BR. + NO
BR29	3.73e-21	1.99e-12	11.90		9	BRNO + BRNO = BR2 + #2 NO
BR30		(Slow)			18	BRNO + O3 = BRNO2 + O2
BR31		Phot Set= CLNO2			19	BRNO2 + HV = BR. + NO2
BR32	6.40e-5	1.00e+15	26.17		20	BRNO2 = BR. + NO2

Table 1 (continued)

Label	Rate Parameters [a]				Refs & Notes [b]	Reaction and Products [c]
	k(298)	A	Ea	B		
BR33	1.75e-15	2.30e-12	4.25		21	BRNO2 + NO = BRNO + NO2
BR34	Phot Set= CLONO				19	BRONO + HV = BR. + NO2
(12)	8.02e-14	2.30e-12	1.99		22	BRONO + NO = BRNO + NO2
BR36	2.00e-16	2.00e-16			23	BRONO + NO2 = BRNO2 + NO2
BR37	2.11e+0	3.37e+12	16.64		24	BRONO = BR. + NO2
BR38	Phot Set= BRONO2				25	BRONO2 + HV = #.71 {BRO. + NO2} + #.29 {BR. + NO3}
BR39	2.72e-5	2.79e+13	24.56		26	BRONO2 = BRO. + NO2
BR40	1.00e-16	1.00e-16			27	BRONO2 + BRNO = BR2 + #2 NO2
BR41	3.00e-19	3.00e-19			26	BRONO2 + NO = BRNO + NO3
Wall Reactions						
HBRW	(Wall Dependent)				28	HBR =
Br. + Base Mechanism Organic Reactions						
BR43	1.16e-12	1.70e-11	1.59		3	BR. + HCHO = HBR + HO2. + CO
BR44	3.88e-12	1.30e-11	0.72		3	BR. + CCHO = HBR + CCO-O2.
BR45	1.07e-11	1.07e-11			29	BR. + RCHO = HBR + RCO-O2.
BR46	Same k as rxn BR45				30,31	BR. + GLY = HBR + #.6 HO2. + #1.2 CO + #.4 RCO-O2. + #-.4 XC
BR47	Same k as rxn BR45				30	BR. + MGLY = HBR + CO + CCO-O2.
BR48	Same k as rxn BR45				30	BR. + BALD = HBR + BZCO-O2.
Br. + Test VOC Reactions						
BR49	7.06e-17	2.86e-10	9.01		32,33	BR. + N-C4 = HBR + #.921 RO2-R. + #.079 RO2-N. + #.413 R2O2. + #.632 CCHO + #.12 RCHO + #.485 MEK + #-0.038 XC
BR50	7.72e-16	7.72e-16			33,34	BR. + N-C6 = HBR + #.775 RO2-R. + #.225 RO2-N. + #.787 R2O2. + #.011 CCHO + #.113 RCHO + #.688 PROD2 + #.162 XC
BR51	1.16e-15	1.16e-15			33,34,35	BR. + CYCC6 = HBR + #.791 RO2-R. + #.209 RO2-N. + #.469 R2O2. + #.193 RCHO + #.598 PROD2 + #.58 XC
BR52	9.65e-16	9.65e-16			33,34	BR. + N-C7 = HBR + #.705 RO2-R. + #.295 RO2-N. + #.799 R2O2. + #.055 RCHO + #.659 PROD2 + #1.11 XC
BR53	1.16e-15	1.16e-15			33,34	BR. + N-C8 = HBR + #.646 RO2-R. + #.354 RO2-N. + #.786 R2O2. + #.024 RCHO + #.622 PROD2 + #2.073 XC
BR54	1.60e-13	1.60e-13			36,37	BR. + ETHENE = RCHO + RO2-R. + #-1 XC

Table 1 (continued)

Label	Rate Parameters [a]				Refs & Notes [b]	Reaction and Products [c]
	k(298)	A	Ea	B		
BR55	3.28e-12	3.28e-12			37,38	BR. + PROPENE = RCHO + RO2-R.
BR56	8.77e-12	8.77e-12			39	BR. + T-2-BUTE = R2O2. + #2 CCHO + RO2-BR.
Organic Bromine-Containing Radical Operators						
BR57	Same k as rxn RRNO				40	RO2-BR. + NO = NO2 + BR.
BR58	Same k as rxn RRH2				40	RO2-BR. + HO2. = ROOH + O2 + #-3 XC
BR59	Same k as rxn RRME				40	RO2-BR. + NO3 = NO2 + O2 + BR.
BR60	Same k as rxn RRN3				40	RO2-BR. + C-O2. = #.5 BR. + #.5 HO2. + #.75 HCHO + #.25 MEOH
BR61	Same k as rxn RRR2				40	RO2-BR. + RO2-R. = #.5 BR. + #.5 HO2.
BR62	Same k as rxn RRR2				40	RO2-BR. + R2O2. = RO2-BR.
BR63	Same k as rxn RRR2				40	RO2-BR. + RO2-N. = #.5 BR. + #.5 HO2. + #.5 {MEK + PROD2} + O2 + XC
BR64	Same k as rxn RRR2				40	RO2-BR. + RO2-BR. = BR.
Propyl Bromide Reactions						
PBOH	1.18e-12	1.18e-12			41	C3-BR + HO. = #.626 RO2-R. + #.042 RO2-N. + #.332 RO2-BR. + #.515 RCHO + #.443 ACET + #-.126 XC

[a] Except as indicated, the rate constants are given by $k(T) = A \cdot (T/300)^{B} \cdot e^{-Ea/RT}$, where the units of k and A are cm^3 $molec^{-1}$ s^{-1}, Ea are kcal mol^{-1}, T is ^oK, and R=0.0019872 kcal mol^{-1} deg^{-1}. The following special rate constant expressions are used: Phot Set = *name*: The absorption cross sections and quantum yields for the photolysis reaction are given in Table 3, where "*name*" indicates the photolysis set used. If a "qy=*number*" notation is given, the number given is the overall quantum yield, which is assumed to be wavelength independent. Falloff: The rate constant as a function of temperature and pressure is calculated using $k(T,M) = \{k0(T)\cdot[M]/[1 + k0(T)\cdot[M]/kinf(T)]\}\cdot F^{Z}$, where $Z = \{1 + [\log_{10}\{k0(T)\cdot[M])/kinf(T)\}]^2\}^{-1}$, [M] is the total pressure in molecules cm^{-3}, F is as indicated on the table, and the temperature dependences of k0 and kinf are as indicated on the table. (Slow): The reaction is assumed to be negligible and is not included in the mechanism. It is shown on the listing for documentation purposes only.

Same k as Rxn *label*: The rate constant is the same as the reaction with the indicated label.

[b] Footnotes are given in Table 2.

[c] Format of reaction listing: "=" separates reactants from products; "*#number*" indicates stoichiometric coefficient, "*#coefficient* { *product list* }" means that the stoichiometric coefficient is applied to all the products listed.

Table 2. Documentation notes for the reactions added to the mechanism to represent bromine-containing compounds.

No.	Note
1	Adjusted to fit the rates of O_3 and HBr consumption in O_3 + HBr dark decay experiments. Note, however, that Mellouki et al (1994) report an upper limit of 3 x 10^{-20} cm^3 $molec^{-1}$ sec^{-1} for this reaction, which is a factor of 20 times lower. Therefore, this reaction may be surface enhanced.
2	Necessary to assume that this reaction is relatively rapid to be consistent with the observation that approximately 2 moles of HBr react for each mole of O_3 in O_3 + HBr dark decay experiments. This is the minimum rate constant for this reaction that is consistent with the results of these experiments. The model is not sensitive to this rate constant when increased above this level because this is predicted to be the major fate of HOBr.
3	Rate constant expression from IUPAC evaluation (Atkinson et al, 1997).
4	Reaction shown to have no effect on model predictions of upper limit of NASA (1997) evaluation is used.
5	Reaction shown to have no effect on model predictions of upper limit of Mellouki et al (1994) is used.
6	Rate constant expression from NASA (1997) evaluation.
7	Absorption cross sections from NASA (2000) evaluation. Unit quantum yields for most energetically favored process is assumed.
8	Absorption cross sections from Calvert and Pitts (1966). Uncertain quantification from a small plot. Unit quantum yields assumed.
9	Rate constant given by Baulch et al (1981). Rate constant for Br + Br reaction is for reaction in N2 at 298K
10	Rate constant from Dolson and Klingshirn (1993).
11	As discussed by Broeske and Zabel (1998) and references therein, the major route is expected to be formation of BRONO. Better fits of model simulations to $BrNO_2$ measurements in Br_2 + NO_x irradiations are obtained if it is assumed that this reaction does not form $BrNO_2$.
12	Reaction is speculative. Rate constant is estimated based on rate constants for similar Br + ClO_x reactions. Reaction probably not important except in certain laboratory systems.
13	Average of rate constant of Orlando and Tyndall (1996) and Harwood et al (1998).
14	Based on absorption cross sections given in the IUPAC evaluation (Atkinson et al, 1997), assuming unit quantum yield. BrO has a banded spectrum, and average absorption cross sections over wavelength intervals are used.
15	This is the upper limit rate constant given by Turnipseed et al (1991). It is necessary to assume that the reaction occurs with this rate constant in order for the model to simulate the amount of HBr consumed when the lights are turned on after O3 and HBr react in the dark. Note that using lower or significantly higher rate constants do not fit the data as well as using this value.
16	The reaction forms BrO_2, which is assumed to decompose rapidly to Br + O_2.
17	Absorption Cross Sections digitized from Loock and Qian (1998). Unit quantum yields assumed.
18	The effect of including this speculative reaction in the mechanism was examined, but including it did not result in improved fits of model simulation to the experiments. This reaction is estimated to be exothermic, but information concerning its rate constant could not be found.

Table 2 (continued)

No.	Note
19	Data on absorption cross sections for $BrNO_2$ or BRONO not found. Assumed to have similar absorption cross sections as $ClNO_2$ or ClONO, respectively, with unit quantum yields assumed. $ClNO_2$ and ClONO absorption cross sections from the IUPAC evaluation (Atkinson et al, 1997).
20	Based on 298 rate constant given by Broeske and Zabel (1998), with estimated A factor based on high pressure limit for N_2O_5 decomposition. Highly approximate and only applicable for 298K and atmospheric pressure.
21	Rate constant from Broeske and Zabel (1998).
22	As discussed by Broeske and Zabel (1998), data indicate that this reaction is faster than $BrNO_2$ + NO, but quantitative information is not available. Assume same A factor as $BrNO_2$ reaction, but half the activation energy.
23	Based on the 298^{o}K rate constant derived by Broeske and Zabel (1998) from a complex chemical system. Probably has a relatively low A factor.
24	Based on line for 1 bar on Figure 3 of Broeske and Zabel (1998). This is for 1 atm pressure only.
25	Absorption cross sections from IUPAC (Atkinson et al, 1997) and NASA (1997) recommendations. Overall quantum yields and mechanism from data cited in NASA (1997) evaluation.
26	Rate constant expression from Orlando and Tyndall (1996).
27	Rate constant is lower limit given by Orlando and Tyndall (1996).
28	The rate constant for this reaction is adjusted to fit rates of HBr decay measured under the conditions of the experiments. This varies with chamber and is significantly enhanced with humidity.
29	Room temperature rate constant for Br + propionaldehyde based on rate constant relative to Br + acetaldehyde at 295K given by Wallington et al (1989), placed on an absolute basis using the IUPAC (Atkinson et al, 1997) recommended rate constant for the reference reaction.
30	Assumed to have the same rate constant as Br. + propionaldehyde.
31	Assumed to have similar mechanism as OH + Glyoxal reaction.
32	Rate constant from Seakins et al (1992), as used in the review by Bierbach et al (1996). Note that the room temperature rate constant is an extrapolation. The mechanism following the H abstraction is assumed to be the same as for the OH reaction.
33	The mechanism following the H abstraction is assumed to be the same as for the OH reaction.
34	The rate constant per CH_2 group is assumed to be the same as for Br. + cyclopentane, which in turn is based on the rate constant relative to Br + isobutane given by Wallington et al (1989), placed on an absolute basis using reference rate constant of Seakins et al (1992), extrapolated to 298K. The mechanism following the H abstraction is assumed to be the same as derived for the OH reaction.
35	The expression for the Br + cyclohexane rate constant relative to Br + n-butane given by Ferguson and Whittle (1971) is not used because it predicts that Br reacts faster with n-butane than with cyclohexane.
36	Room temperature rate constant from Barnes et al (1989).

Table 2 (continued)

No.	Note
37	Mechanism assumed to involve the initial addition of Br to the double bond, with the resulting alkoxy radical primarily reacting with O2 to form HO_2 and the corresponding brominated aldehyde, which is represented by the lumped higher aldehyde (RCHO) model species.
38	Average of room temperature rate constants of Barnes et al (1989) and Wallington et al (1989).
39	Room temperature rate constant is average of the rate constants tabulated by Bierbach et al (1996). The mechanism is assumed to involve the initial addition of Br to the double bond, with the resulting alkoxy radical formed after addition of O_2 and reaction with NO being estimated to primarily decompose to acetaldehyde and $\cdot CH_2Br$ radicals. The latter are assumed to form formaldehyde and Br atoms after addition of O_2, reaction with NO, and decomposition of the alpha-bromo alkoxy radical.
40	RO2-BR. represents formation of peroxy radicals that react with NO to form bromine atoms. Its reactions with other species is analogous to the treatment of RO2-R in the base mechanism, except that Br is formed in place of HO2 in reactions where HO_2 is formed.
41	The mechanism is based on that of Carter et al (1997), except the lumped higher aldehyde is used to represent bromine-substituted aldehydes. Likewise, acetone (ACET) is used to represent bromoacetone. As discussed by Carter et al (1997), assuming the bromine-substituted aldehydes react significantly different from other aldehydes does not result in significant improvements to model predictions.

these runs was that derived by Carter et al (1995) based on spectral measurements made in 1989. The appropriateness of using this spectrum was evaluated by measuring the spectrum of the light in this chamber during the course of this program using a LiCor LI-1800 spectroradiometer, and the results were found to be essentially the same. Use of the Carter et al (1995) EC spectrum is preferred over the LiCor spectrum taken during this project because of the greater resolution of the former.

Except as indicated, the chamber effects model used when modeling the EC runs in this report is the same as that used by Carter (2000) when modeling earlier runs carried out in this chamber. A dark decay reaction for HBr was added, with rates based on the results of the HBr dark decay experiments as discussed in this report. Although the standard wall effects model for smog simulation experiments in the EC assumes that a portion of the injected NO_2 is converted to HONO during the injection process, this is assumed not to be the case for these experiments. This is because the NO_2 injections in these experiments employed vacuum methods under very dry conditions, and if initial HONO formation did occur it would have been detected by FT-IR in the experiments employing high concentrations of NO_2. No initial HONO was detected in any of the experiments carried out for this project.

Table 3. Absorption cross sections and quantum yields used to calculate photolysis rates of photoreactive bromine-containing species.

WL (nm)	Abs (cm^2)	QY	WL (nm)	Abs (cm^2)	QY	WL (nm)	Abs (cm^2)	QY	WL (nm)	Abs (cm^2)	QY	WL (nm)	Abs (cm^2)	QY
							HOBR							
250.0	4.15e-20	1.000	255.0	6.19e-20	1.000	260.0	1.05e-19	1.000	265.0	1.46e-19	1.000	270.0	1.87e-19	1.000
275.0	2.21e-19	1.000	280.0	2.43e-19	1.000	285.0	2.50e-19	1.000	290.0	2.40e-19	1.000	295.0	2.19e-19	1.000
300.0	1.91e-19	1.000	305.0	1.62e-19	1.000	310.0	1.36e-19	1.000	315.0	1.18e-19	1.000	320.0	1.08e-19	1.000
325.0	1.05e-19	1.000	330.0	1.08e-19	1.000	335.0	1.13e-19	1.000	340.0	1.19e-19	1.000	345.0	1.23e-19	1.000
350.0	1.24e-19	1.000	355.0	1.21e-19	1.000	360.0	1.15e-19	1.000	365.0	1.05e-19	1.000	370.0	9.32e-20	1.000
375.0	7.99e-20	1.000	380.0	6.65e-20	1.000	385.0	5.38e-20	1.000	390.0	4.22e-20	1.000	395.0	3.23e-20	1.000
400.0	2.43e-20	1.000	405.0	1.80e-20	1.000	410.0	1.36e-20	1.000	415.0	1.08e-20	1.000	420.0	9.67e-21	1.000
425.0	9.98e-21	1.000	430.0	1.15e-20	1.000	435.0	1.40e-20	1.000	440.0	1.68e-20	1.000	445.0	1.96e-20	1.000
450.0	2.18e-20	1.000	455.0	2.29e-20	1.000	460.0	2.28e-20	1.000	465.0	2.14e-20	1.000	470.0	1.91e-20	1.000
475.0	1.62e-20	1.000	480.0	1.30e-20	1.000	485.0	9.93e-21	1.000	490.0	7.23e-21	1.000	495.0	5.02e-21	1.000
500.0	3.33e-21	1.000	505.0	2.12e-21	1.000	510.0	1.29e-21	1.000	515.0	7.60e-22	1.000	520.0	4.20e-22	1.000
525.0	2.30e-22	1.000	530.0	1.20e-22	1.000	535.0	5.90e-23	1.000	540.0	2.90e-23	1.000	545.0	1.30e-23	1.000
550.0	6.00e-24	1.000	555.0	0.00e+00										
							BR2							
200.0	1.91e-20	1.000	300.0	3.82e-21	1.000	330.0	3.82e-21	1.000	350.0	3.82e-20	1.000	400.0	4.97e-19	1.000
410.0	6.31e-19	1.000	430.0	6.31e-19	1.000	450.0	4.59e-19	1.000	500.0	3.06e-19	1.000	520.0	1.53e-19	1.000
550.0	7.65e-20	1.000	600.0	7.65e-21	1.000	650.0	0.00e+00	1.000						
							BRO							
300.0	2.00e-18	1.000	304.9	2.00e-18	1.000	305.1	2.59e-18	1.000	309.9	2.59e-18	1.000	310.1	4.54e-18	1.000
314.9	4.54e-18	1.000	315.1	3.91e-18	1.000	319.9	3.91e-18	1.000	320.1	6.00e-18	1.000	324.9	6.00e-18	1.000
325.1	7.53e-18	1.000	329.9	7.53e-18	1.000	330.1	6.28e-18	1.000	334.9	6.28e-18	1.000	335.1	5.89e-18	1.000
339.9	5.89e-18	1.000	340.1	5.15e-18	1.000	344.9	5.15e-18	1.000	345.1	3.99e-18	1.000	349.9	3.99e-18	1.000
350.1	2.28e-18	1.000	354.9	2.28e-18	1.000	355.1	1.72e-18	1.000	359.9	1.72e-18	1.000	360.1	1.61e-18	1.000
364.9	1.61e-18	1.000	365.1	9.20e-19	1.000	369.9	9.20e-19	1.000	370.1	5.10e-19	1.000	374.9	5.10e-19	1.000
375.0	0.00e+00	1.000												
							BRNO							
250.0	1.21e-17	1.000	280.0	3.82e-19	1.000	300.0	5.79e-19	1.000	350.0	5.79e-19	1.000	400.0	4.10e-19	1.000
450.0	3.04e-19	1.000	500.0	1.71e-19	1.000	550.0	6.80e-20	1.000	600.0	1.92e-20	1.000	650.0	1.92e-20	1.000
700.0	6.06e-20	1.000	720.0	6.06e-20	1.000	800.0	1.52e-20	1.000	900.0	3.82e-22	1.000			
							CLNO2							
190.0	2.69e-17	1.000	200.0	4.68e-18	1.000	210.0	3.20e-18	1.000	220.0	3.39e-18	1.000	230.0	2.26e-18	1.000
240.0	1.33e-18	1.000	250.0	9.06e-19	1.000	260.0	6.13e-19	1.000	270.0	3.53e-19	1.000	280.0	2.20e-19	1.000
290.0	1.73e-19	1.000	300.0	1.49e-19	1.000	310.0	1.21e-19	1.000	320.0	8.87e-20	1.000	330.0	5.84e-20	1.000
340.0	3.54e-20	1.000	350.0	2.04e-20	1.000	360.0	1.15e-20	1.000	370.0	6.90e-21	1.000	380.0	0.00e+00	1.000
							CLONO							
235.0	2.15e-18	1.000	240.0	1.76e-18	1.000	245.0	1.37e-18	1.000	250.0	1.06e-18	1.000	255.0	6.50e-19	1.000
260.0	6.46e-19	1.000	265.0	6.93e-19	1.000	270.0	9.03e-19	1.000	275.0	1.10e-18	1.000	280.0	1.32e-18	1.000
285.0	1.44e-18	1.000	290.0	1.44e-18	1.000	295.0	1.42e-18	1.000	300.0	1.29e-18	1.000	305.0	1.14e-18	1.000
310.0	1.05e-18	1.000	315.0	9.81e-19	1.000	320.0	8.03e-19	1.000	325.0	7.54e-19	1.000	330.0	5.87e-19	1.000
335.0	5.77e-19	1.000	340.0	4.37e-19	1.000	345.0	3.57e-19	1.000	350.0	2.69e-19	1.000	355.0	2.29e-19	1.000
360.0	1.61e-19	1.000	365.0	1.13e-19	1.000	370.0	9.00e-20	1.000	375.0	6.90e-20	1.000	380.0	4.10e-20	1.000
385.0	3.30e-20	1.000	390.0	2.20e-20	1.000	395.0	1.50e-20	1.000	400.0	6.00e-21	1.000	405.0	0.00e+00	1.000
							BRONO2							
186.0	1.50e-17	1.000	190.0	1.30e-17	1.000	195.0	1.00e-17	1.000	200.0	7.20e-18	1.000	205.0	4.30e-18	1.000
210.0	3.20e-18	1.000	215.0	2.70e-18	1.000	220.0	2.40e-18	1.000	225.0	2.10e-18	1.000	230.0	1.90e-18	1.000
235.0	1.70e-18	1.000	240.0	1.30e-18	1.000	245.0	1.00e-18	1.000	250.0	7.80e-19	1.000	255.0	6.10e-19	1.000
260.0	4.80e-19	1.000	265.0	3.90e-19	1.000	270.0	3.40e-19	1.000	275.0	3.10e-19	1.000	280.0	2.90e-19	1.000
285.0	2.70e-19	1.000	290.0	2.40e-19	1.000	295.0	2.20e-19	1.000	300.0	1.90e-19	1.000	305.0	1.80e-19	1.000
310.0	1.50e-19	1.000	315.0	1.40e-19	1.000	320.0	1.20e-19	1.000	325.0	1.10e-19	1.000	330.0	1.00e-19	1.000
335.0	9.50e-20	1.000	340.0	8.70e-20	1.000	345.0	8.50e-20	1.000	350.0	7.70e-20	1.000	360.0	6.20e-20	1.000
370.0	4.90e-20	1.000	380.0	4.00e-20	1.000	390.0	2.80e-20	1.000	400.0	0.00e+00	1.000			

RESULTS AND DISCUSSION

Summary of Experiments

The experiments carried out for this program included HBr dark decay determinations, experiments where HBr is reacted with O_3, NO_x, and/or formaldehyde in the dark and upon irradiation, and experiments where Br_2 is irradiated in the presence of NO_x and/or formaldehyde. In addition, two NO_2 actinometry were carried out to measure the intensity of the light source used in these experiments, and the spectrum of the light source was also measured.

A chronological listing of all the experiments carried out for this program is given on Table 4, which gives a summary of the procedures for the experiments and the major results. Detailed tabulations of the data obtained are given in Appendix A to this report. Figures and tables showing selected results are given where applicable in the discussion below, usually with comparisons with results of model simulations.

Light Characterization Results

As indicated on Table 4, two NO_2 actinometry experiments were carried out during this project. These involved the irradiation of NO_2 in N_2 and monitoring the formation of NO. The results of both experiments indicated an NO_2 photolysis rate of 0.12 min^{-1}. This value was obtained by conducting model simulations of the experiments and using the NO_2 photolysis rate that gave the best fits of the model simulations to the experimental NO_2 and NO profiles. This NO_2 photolysis rate was used, in conjunction with a light source spectrum for this chamber, to calculate the rates of all the photolysis reactions when modeling the experiments for this program, given the absorption cross sections and quantum yields. The light source spectrum was measured during the course of this program using a LiCor LI-1800 spectroradiometer, and the spectrum was essentially the same as that given by Carter et al (1995), which was used when modeling the experiments discussed in this report.

HBr Dark Decay

Table 5 gives a summary of all the HBr dark decay rate measurements made during the experiments for this program, including runs when reactants other than O_3 are present. (The experiments with O_3 present are discussed in the following section) Decay rates measured in the presence of formaldehyde, NO, NO2 and nitric acid are also shown, as well as for the two runs where humidity was varied.

Table 4. Summary of experiments carried out for this project

Run	Run Type	Procedure	Results
EC1767	HBr Dark and Light Decay	Approximately 20 ppm of HBr injected into the chamber and its dark and then light decay was monitored.	The dark decay rate was 6.3×10^{-4} min^{-1}, and the light decay was essentially the same, at 6.7×10^{-4} min^{-1}.
EC1768	HBr + O_3 (Dark)	Approximately 20 ppm each HBr and O_3 injected and monitored in the dark.	Both O_3 and HBr reacted, but not to completion. Results are shown on Table 6.
EC1769	HBr + O_3 (Dark + Light)	(1) Approximately 20 ppm HBr injected and reaction monitored. (2) 20 ppm O_3 added and reaction monitored. (3) Lights turned on and reaction monitored. (4) Additional 20 ppm O_3 added when lights on.	(1) Both O_3 and HBr reacted in the dark, but not to completion. (2) All the O_3 disappeared when the lights were turned on, but HBr declined only slightly. (3) When O_3 was injected again, all the O_3 was immediately reacted, but HBr declined only slightly. Results are shown on Figure 1 and Table 6
EC1770	HBr + NO (Dark + Light)	(1) HBr injected and its decay was monitored in the dark. (2) NO injected and the reactants were monitored in the dark. (3) The lights were turned on and the reactants were monitored.	(1 and 2) NO injection did not significantly affect the HBr decay. NO declined due to its oxidation to NO2 (which was not monitored). (3) HBr decay increased slightly when lights turned on, but NO consumption ended. Results are shown on Figure 1.
EC1772	HCHO + HBr + O_3 (Dark + Light)	(1) Approximately 7 ppm HCHO and 20 ppm HBr injected and monitored in the dark. (2) O3 added and reactants monitored in the dark. (3) Lights turned on for brief periods and reactants measured during intervening intervals.	(1) No significant reaction in absence of O_3. (2) Relatively slow decay of O_3 and HBr in the dark, with no significant consumption of HCHO. (3) Turning on the lights caused O_3 and HCHO to be consumed and CO to be formed, but no apparent effect on rate of HBr consumption. Results are shown on Figure 2.
EC1773	HBr + O_3 (Dark + Light)	(1) Approximately 10 ppm of HBr and 20 ppm O3 reacted in dark. (2) Lights turned on for short intervals and reactants monitored.	(1) Slow consumption of O_3 and faster consumption of HBr, with most of the HBr and only a little of the O_3 consumed by the time the lights turned on. (2) The remaining O_3 rapidly disappeared when lights turned on. Results are shown on Figure 1 and Table 6.

Table 4 (continued)

Run	Run Type	Procedure	Results
EC1774	HBr + NO_2 (Dark + Light)	(1) Approximately 20 ppm HBr and 10 ppm NO_2 monitored in the dark. (2) Lights turned on and reactants monitored.	(1) No apparent dark reaction. HBr consumption only slightly greater than normal dark decay rate. (2) Turning on lights caused HBr consumption to increase and NO_2 to decrease and NO to be formed, though not particularly rapidly. Results are shown on Figure 6.
EC1775	HBr + HCHO + NO_2	(1) 7 Approximately 7 ppm HCHO, 20 ppm HBr and 10 ppm NO_2 injected and monitored in the dark. (2) Lights turned on and reactants monitored.	(1) No apparent dark reaction. HBr consumption approximately at normal dark decay rate. (2) Turning on lights caused NO_2, HBr, and HCHO to be consumed at moderate rates, and NO and CO to be formed. Results are shown on Figure 8.
EC1776	HBr + O_3 + HCHO (HBr added in light).	(1) Approximately 20 ppm O_3 and 7 ppm HCHO injected and lights turned on and reactants monitored. (2) Approximately 10 ppm HBr injected while lights on and reactants monitored.	(1) O_3 and HCHO were consumed at moderate rates and CO formation observed. (2) Injecting the HBr caused the O_3 and HCHO to be rapidly consumed and approximately half the added HBr to react. Results are shown on Figure 3 and Figure 4.
EC1777	HBr + O_3 + HCHO (HBr added in light).	Essentially the same procedure and injection amounts as EC1776.	Similar results to EC1776 except much slower reaction rates after HBr was injected. Results are shown on Figure 3 and Figure 4.
EC1778	HBr + O_3 (Dark + Light)	Similar procedures and amounts of reactants injected as run EC1773. Modified IR analysis method employed to permit detection of HOBr.	Similar results as EC1773, except that HOBr was also detected during the dark reaction period, though not quantified. Results are shown on Figure 1 and Table 6.
EC1779	HBr + NO_2 (Dark + Light)	(1) Approximately 8 ppm HBr and 10 ppm NO_2 injected and monitored in the dark. (2) Lights turned on and reactants monitored.	(1) No apparent dark reaction. (2) NO_2 converted to NO and consumption rate of HBr increased. Small amounts of BrNO observed in both dark and light. Results are shown on Figure 6.

Table 4 (continued)

Run	Run Type	Procedure	Results
EC1780	HBr + NO (light)	(1) Approximately 10 ppm of HBr and 9 ppm of NO injected and monitored in the dark. (2) Lights turned on and reactants monitored.	(1) NO oxidized to NO_2 at expected rate in the dark. Decay rate of HBr somewhat greater than indicated by previous dark decay determinations. BrNO was observed to continuously increase. (2) Turning on the lights stopped the NO to NO_2 conversion and significantly reduced the level of BrNO (but not to zero), but did not significantly affect the HBr consumption rate. Results are shown on Figure 6.
EC1781	HBr + O_3 (dark)	(1) Approximately 4 ppm of HBr and 20 ppm of O_3 injected and monitored. (2) Subsequent injections of first 4 ppm then 8 ppm of HBr were added, and reactants monitored after each injection.	The O_3 decayed only slowly, but the HBr reacted at a moderate rate after each injection. BrNO was not detected except for trace amounts after the last HBr injection. Results are shown on Figure 1 and Table 6.
EC1782	HBr + O_3 + HCHO (light only)	(1) Approximately 6 ppm of HCHO and 17 ppm O_3 injected, lights turned on, and HBr added about 1 minute after lights turned on. Reactants monitored.	O_3 and formaldehyde declined and CO formed until both the O_3 and HCHO were reacted in about 20 minutes. The HBr was consumed relatively slowly for the first 10 minutes and then reacted more rapidly. Results are shown on Figure 4.
EC1783	Br_2 + HCHO (light)	Approximately 6 ppm of HCHO and Br_2 were injected, then the lights were turned on intermittently for brief periods, with reactants monitored. Due to a recording error, the amount of Br_2 added is uncertain, but it is expected to be either 3 or 6 ppm.	Br_2 could not be monitored with the available methods. HCHO reacted each time the lights were turned on, and formation of HBr, CO, H_2O_2 and formic acid were observed. Results are shown on Figure 5.
EC1784	NO_2 Actinometry	NO2 injected in N_2 (with O_2 less than 12 ppm), and lights turned on.	NO_2 consumption rate corresponded to an NO_2 photolysis rate of 0.12 min^{-1}.
EC1785	Br_2 + HCHO (light)	Same procedures as EC1783 except that 3 ppm of Br_2 was added.	Similar results as EC1783 except the HCHO consumption rate and the product yields were about half as much. Results are shown on Figure 5.

Table 4 (continued)

Run	Run Type	Procedure	Results
EC1786	Br_2 + NO_2 (light)	About 5 ppm each of bromine and NO_2 were injected into the chamber, and then irradiated at 30 and 60 second intervals, and then continuously.	There was no apparent reaction between Br_2 and NO_2 in the dark. Slow NO_2 consumption and NO formation was observed upon continuous irradiation. Trace levels of BrNO and $BRNO_2$ were observed once the irradiation began. Results are shown on Figure 7.
EC1787	Br_2 + NO (light)	About 10 ppm of NO and 5 ppm of Br_2 were injected into the chamber, and then irradiated during several 30 second intervals and then continuously.	Similar results as EC1786. Relatively slow conversion of NO to NO_2 was observed upon irradiation. Traces of BrNO and $BRNO_2$ were observed to be formed during the initial irradiation period, and then stay at relatively constant levels during continued irradiation. Results are shown on Figure 7.
EC1788	Br_2 + Dimethyl Ether (light)	Run carried out to determine whether Br reacted with diethyl ether, to investigate its potential use as an OH radical tracer. About 5 ppm each of Br_2 and diethyl ether were irradiated intermittently.	Diethyl ether was consumed and HBr was formed at a slightly higher level than the amount of diethyl ether reacted. Ethyl formate, an expected reaction product from H-abstraction reactions from diethyl ether, was observed, though in lower yield than the amount of ether reacted.
EC1789	Br_2 + aromatics (light)	Run carried out to determine whether Br reacted with aromatics, to investigate their potential use as an OH radical tracer. About 5 ppm each of Br_2 and p-xylene and 3 ppm 1,3,5-trimethylbenzene were irradiated intermittently then continuously.	Both aromatics were consumed and HBr was formed at somewhat higher yields than the amount of aromatics reacted. 1,3,5-trimethylbenzene reacted a factor of 1.4 times faster than p-xylene, as expected if most of the reaction is abstraction from a methyl group.
EC1790	HBr + HNO_3 (dark)	Approximately 20 ppm of HBr was injected and its dark decay was measured. Then approximately 10 ppm of HNO_3 was injected and the dark decay of each were monitored.	The HBr decay rate before the HNO_3 was added was about 5% per hour, which is slightly greater than the average HBr decay rate of ~4% per hour. The addition of HNO_3 caused the HBr decay rate to slow to ~2% per hour. The HNO_3 decay rate was also ~2% per hour. See Table 5.

Table 4 (continued)

Run	Run Type	Procedure	Results
EC1791	Br_2 + Alkanes (light)	Run carried out to determine whether Br reacted with alkanes, to investigate their potential use as an OH radical tracer. About 10 ppm of Br_2 and 5 ppm each of cyclohexane and 2,3-dimethylbutane were irradiated intermittently then continuously.	Very slow consumption of cyclohexane and somewhat more rapid consumption of 2,3-dimethylbutane was observed. If Br reaction is the only consumption process for each, the rate constant for Br reaction with 2,3-dimethylbutane is determined to be about 10.5 times faster than its reaction with cyclohexane.
EC1792	HBr + O_3 + Alkane tracer (Dark + Light)	About 20 ppm of HBr and O_3 were reacted in the dark and then the lights were turned on. 0.3 ppm of cyclohexane was added as an OH radical tracer, but no useful cyclohexane data were obtained because of analytical problems. A second injection of 20 ppm of O_3 was made during the irradiation.	O_3 and HBR reacted in the dark, though at a somewhat slower rate than in previous runs. Turning on the lights caused all the O_3 to disappear and the HBr to decrease slightly. The second O_3 injection caused all the O_3 to be rapidly consumed and a slight decrease in HBr. Results are shown in Figure 1.
EC1793	NO_2 Actinometry	Approximately 5 ppm of NO_2 was irradiated in N_2 in the presence of less than 3 ppm O_2.	The results were consistent with the results of the previous actinometry experiment and indicated a NO_2 photolysis rate of 0.12 min^{-1}.
EC1795	Br_2 + NO_2 + HCHO + Alkane tracer (light)	6 ppm of formaldehyde, 5 ppm of NO_2, 3 ppm Br_2 and 0.3 ppm n-heptane tracer were added and irradiated intermittently.	About 1 ppm of HBr was formed after the first irradiation, and did not increase during subsequent irradiations. Some formaldehyde and lesser amounts of NO_2 were reacted during each irradiation. About 3% of the n-heptane tracer was consumed during the first irradiation, and no subsequent consumption was observed. Formation of CO, CO_2, formic acid, HNO_3, N_2O_5, HO_2NO_2, HONO, and trace amounts of BRNO and $BrNO_2$ were observed. Results are shown on Figure 9.
EC1796	HBr + O_3 + Tracer (light)	This was essentially a repeat of EC1792, except that this time useable cyclohexane data were obtained.	The O_3 and HBr results were similar to run EC1792. Approximately 20% of the cyclohexane was consumed when the lights were turned on, but the consumption during the second O_3 addition was relatively minor. Results are shown on Figure 1.

Table 4 (continued)

Run	Run Type	Procedure	Results
EC1797	HBr + O_3 + HCHO + Tracer (light)	About 7 ppm formaldehyde, 20 ppm O_3 and 0.5 ppm cyclohexane tracer were irradiated. After about 45 minutes, 10 ppm HBr was added with the lights still on.	Both O_3 and formaldehyde reacted at a moderate rate while the lights were on prior to the HBr addition, consistent with previous such experiments. The cyclohexane tracer declined about 25% during this period, indicating the presence of OH radicals. After the addition of HBr, both the O_3 and formaldehyde were consumed after about 5 minutes, and the cyclohexane was reacted by another 10%. Once the O_3 and formaldehyde reacted no further cyclohexane consumption occurred. CO was formed as the formaldehyde reacted. Results are shown on Figure 4.
EC1798	HBr + O_3 (25% RH, dark)	20 ppm of HBr was added to the chamber humidified to 25% RH and its dark decay was monitored. Then 20 ppm O_3 was added and both were monitored.	The HBr dark decay rate was 78% per hour, or about a factor of 20 times higher than the dark decay rate of ~4% per hour. The addition of the O_3 caused the HBr decay to increase and O_3 also slowly decreased. Results are shown on Figure 1 and Table 5.
EC1799	HBr + O_3 (13% RH, dark)	20 ppm of HBr was added to the chamber humidified to13% RH and its dark decay was monitored. Then 20 ppm O_3 was added and both were monitored.	The HBr dark decay rate was 19% per hour, or about a factor of 5 times higher than the dark decay rate of ~4% per hour. The addition of the O_3 caused the HBr decay to increase and O_3 also slowly decreased. Results are shown on Figure 1 and Table 5.

The results indicate an average HBr dark decay rate in dry air in this chamber of ~4% per hour in the absence of other reactants, with a standard deviation of about 25%. The decay rates are significantly higher in the humidified experiments, increasing by a factor of ~5 when the humidity is increased to 13%, and by a factor of ~20 when increased to 25%. Thus these data suggest that the HBr decay rate increase with approximately the square of the humidity, at least in the ≤25% humidity range.

Effects of Added Reactants on the HBr Dark Decay Rate

Table 5 shows that the presence of NO, formaldehyde, and nitric acid slightly slow the dark decay rate, though the difference may not be significant except perhaps for HNO_3, where a decay rate was

Table 5. Summary of HBr dark decay rates.

Run	Other Reactants	Dark Decay Rate (% per hour)
EC-1767	Dry Air	3.8%
EC-1768	Dry Air	2.4%
EC-1773	Dry Air	4.2%
EC-1774	Dry Air	3.9%
EC-1790	Dry Air	5.0%
Average of above		3.9±0.9%
EC-1772	HCHO (7 ppm)	2.3%
EC-1770	NO (8 ppm)	2.9%
EC-1775	NO_2 (10 ppm) + HCHO (7 ppm)	5.5%
EC-1779	NO_2 (10 ppm)	9.3%
EC-1790	HNO_3 (10 ppm)	2.2%
EC-1799	13% RH	19.3%
EC-1798	25% RH	78.3%

determined both before and after HNO_3 addition. This indicates that there is no significant gas phase reaction between HBr and these compounds, and they may be slightly deactivating the walls for HBr absorption.

On the other hand, Table 5 shows that the presence of ~10 ppm of NO_2 appears to cause a non-negligible enhancement in the HBr dark decay rate. Slow decays of NO_2 also occur in these experiments, suggesting that a reaction may be occurring. After correcting for HBr wall losses based on the results of the experiments in the absence of other reactants, the excess HBr decay rates in the presence of ~10 ppm of NO_2 correspond to apparent HBr + NO_2 rate constants of 1.8 and 6 x 10^{-20} cm^3 $molec^{-1}$ s^{-1}, with the lower apparent experiment being derived for the experiment where formaldehyde is also present. The numbers of molecules of HBr consumed per molecule of NO_2 consumed are respectively 1.7 and 0.9 for the two experiments. The variability of these results suggests that this enhanced decay may be a wall process. Because of this and the low apparent overall rate constant, this process is ignored in the modeling of the experiments discussed in this report.

HBr + O_3 Dark Reactions

The addition of O_3 to HBr (or vise-versa) caused both to be consumed at rates that are significantly greater than their dark decay rates in the absence of other reactants, indicating that these compounds undergo a non-negligible dark reaction. Table 6 gives a summary of the conditions and results

of the experiments where O_3 and HBr were reacted in the dark, indicating the overall O_3 + HBr and overall reaction stoichiometry (molecules of HBr consumed per molecule of O_3 reacted) that best fit the data. These were obtained as indicated on the footnote to the table.

The best fit rate constants on Table 6 showed no obvious dependence on reaction condition, including humidity. The average of the best fit rate constants derived from these data was (4.1±1.3) x 10^{-19} cm^3 $molec^{-1}$ s^{-1}. On the average, 2.4±0.4 moles of HBr were consumed for each mole of O_3 reacted, after correcting for the dark wall losses for each reactant in the absence of the other. The ratio of HBr to O_3 reacted had a small apparent dependence on the HBr levels, averaging 2.5±0.2 in the runs with less than 10 ppm initial HBr, and 2.2±0.3 in the runs with lower HBr levels. However, given the scatter of the data, that difference may not be significant. As with the overall rate constant, the ratio of HBr to O_3 reacted had no apparent humidity dependence.

The lack of humidity dependence suggests – though it does not prove – that the O_3 + HBr reaction may be occurring in the gas phase rather than on the walls of the chamber. If it were a wall-mediated process, one would think humidity would significantly affect the rate, especially considering the large effect of humidity on the rate of HBr absorption on the wall, as indicated in the previous section. On the other hand, the apparent O_3 + HBr rate constant obtained in this work is inconsistent with the results of Mellouki et al (1994), who report an upper limit of 3 x 10^{-20} cm^3 $molec^{-1}$ s^{-1} for this reaction. The reason for this discrepancy is unknown, and tends to suggest, contrary to the indication from these humidity experiments, that the process may in fact be wall mediated.

The fact that more than one molecule of HBr is consumed for each molecule of O_3 reacted indicates that more than one reaction is taking place. If the reaction is assumed to be occurring in the gas phase, the most reasonable explanation is to assume that the initial process is formation of HOBr, which then reacts to consume an additional molecule of HBr, as follows:

$$O_3 + HBr \rightarrow HOBr + O_2 \quad (1)$$

$$HOBr + HBr \rightarrow Br_2 + H_2O \quad (2)$$

If this is assumed, and a rate constant of

$$k_1 = 4.1 \times 10^{-19} \text{ cm}^3 \text{ molec}^{-1} \text{ s}^{-1}$$

is used based on the fits to the O_3 + HBr dark experiments as shown on Table 6, then it is also necessary to assume that

$$k_2 \geq 3.5 \times 10^{-15} \text{ cm}^3 \text{ molec}^{-1} \text{ s}^{-1.}$$

in order for model simulations to approximately fit the HBr loss rates.

There is no direct information on whether HOBr indeed reacts as rapidly with HBr in the gas phase as indicated in this work. However, the reaction is observed to occur on water ice at low temperature, and Br_2 is observed to be formed as a product (Abbatt, 1994, NASA, 1997). The formation of Br_2 in the dark reaction is also consistent with the results of the experiments where the HBr + O_3 mixtures were subsequently irradiated, as discussed below. Therefore, this is not an unreasonable reaction to assume, though it may be occurring on the walls.

Although Reaction (1) was used by Carter et al (1997) to fit the alkyl bromide reactivity data, the rate constant used in that work was approximately 10^{-15} cm^3 $molec^{-1}$ s^{-1}, which is over 10^3 times higher. Reaction (2) was not considered in the analysis of Carter et al (1997). If these are surface reactions, they would be expected to be slower in the experimental system of Carter et al (1997) than in that used in these experiments. This is because the FEP Teflon film used in that work tends to have lower surface effects than the Teflon-coated metal and Pyrex surfaces of the EC used in this study (Carter et al, 1995, and references therein).

Figure 1 shows the experimental and calculated concentration-time plots measured in the experiments where O_3 was reacted with HBr in the absence of other reactants. The data obtained prior to ozone addition are shown for the humidified runs (EC1799 and EC1798) but not for the other runs. The discontinuities in the data for the runs on the bottom half of the figure indicate when the lights were turned on; these data are discussed in the following section. In general, the model fit the ozone decay reasonably well in these experiments, though it tended to underpredict the rates of HBr reaction compared to O_3 reaction. This is because, as shown on Table 6, the data indicate that somewhat more than two moles of HBr react for each mole of O_3 reacted, while the model, which represents these processes by Reactions (1) and (2) only, predicts an upper limit of two for this ratio.

HBr + O_3 Light Reactions

Experimental and calculated concentration-time data for the experiments where O_3 + HBr mixtures were irradiated are shown on the bottom half of Figure 1. In all these experiments the lights were turned on after reacting O_3 and HBr in the dark for a period, and this resulted in a rapid consumption of all the O_3 present, and a rapid but slight decreases in HBr levels. Second injections of O_3 were made in runs EC1792 and EC1796, and in both cases the added O_3 was rapidly consumed, and a rapid but slight consumption of HBr also occurred. Run EC1796 had cyclohexane present as a radical tracer, whose consumption could serve as an indicator of radicals which might react with it. No consumption of cyclohexane was observed during the dark portion of the experiment, but slight but measurable amounts of cyclohexane reacted when the O_3 was injected.

The rapid consumption of O_3 when the lights are turned on is consistent with model predictions. It is attributed to the formation of Br_2 in the dark due to Reaction (2), above, which then rapidly photolyzes to form Br atoms when the lights are turned on, with the Br atoms then rapidly reacting with

Table 6. Summary of conditions and major results of the experiments where O_3 and HBr were reacted in the dark.

Run	Initial Conc (ppm)		Best Fit [a]	
	HBr	O3	k(O_3+HBr) (cm^3 $molec^{-1}$ s^{-1})	O_3 / HBr React Ratio.
EC1781 (initial)	3.49	19.11	5.7e-19	2.6
EC1781 (2nd HBr addition)	3.88	17.16	3.6e-19	2.7
EC1781 (3rd HBr Addition)	8.11	15.15	3.6e-19	2.6
EC1773	8.03	18.34	4.6e-19	2.3
EC1778	8.70	18.93	3.4e-19	2.5
EC1769	16.54	15.25	4.6e-19	2.5
EC1768	16.63	14.49	5.9e-19	2.5
EC1792	17.65	18.05	2.2e-19	2.3
EC1796	18.01	19.33	2.2e-19	2.2
EC1799 (13% RH)	13.23	19.65	4.1e-19	1.7
EC1798 (25% RH)	6.48	19.05	5.6e-19	2.3

[a] The best fit rate constants and reaction stoichiometry ratios were obtained by fitting the data with the model: $d[O_3]/dt = k\,[O_3][HBr] - k_{wall}^{O3}\,[O_3]$; $d[HBr]/dt = \alpha \cdot k\,[O_3][HBr] - k_{wall}^{HBr}\,[HBr]$, where k is the O_3 + HBr rate constant, α is the molecules HBr reacted per molecule O_3 reacted, and k_{wall}^{O3} and k_{wall}^{HBr} are the dark decay rates of O_3 and HBr in the absence of other reactants. For O_3, an average dark decay rate of 7.8×10^{-4} min^{-1} was used, based on O_3 decay rates observed in the absence of other reactants. For HBr, the dark decay rates for the dry experiments were the average of those obtained in dry experiments as shown on Table 5, while for the humidified experiments the HBr dark decay rates measured prior to the O_3 addition were used.

the O_3. Under the conditions of these experiments, the photolytic half-life of Br_2 is calculated to be 1.6 minutes. The reactions that are predicted to be the most important under these conditions are as follows:

$$Br_2 + h\nu \rightarrow Br + Br \quad (3)$$

$$Br + O_3 \rightarrow BrO + O_2 \quad (4)$$

$$BrO + BrO \rightarrow Br + Br + O_2 \quad (5)$$

$$BrO + BrO \rightarrow Br_2 + O_2 \quad (6)$$

$$BrO + HBr \rightarrow Br_2 + OH \quad (7)$$

$$OH + Br_2 \rightarrow HOBr + Br \quad (8)$$

$$OH + HBr \rightarrow H_2O + Br \quad (9)$$

$$HOBr + HBr \rightarrow Br_2 + H_2O \quad (2)$$

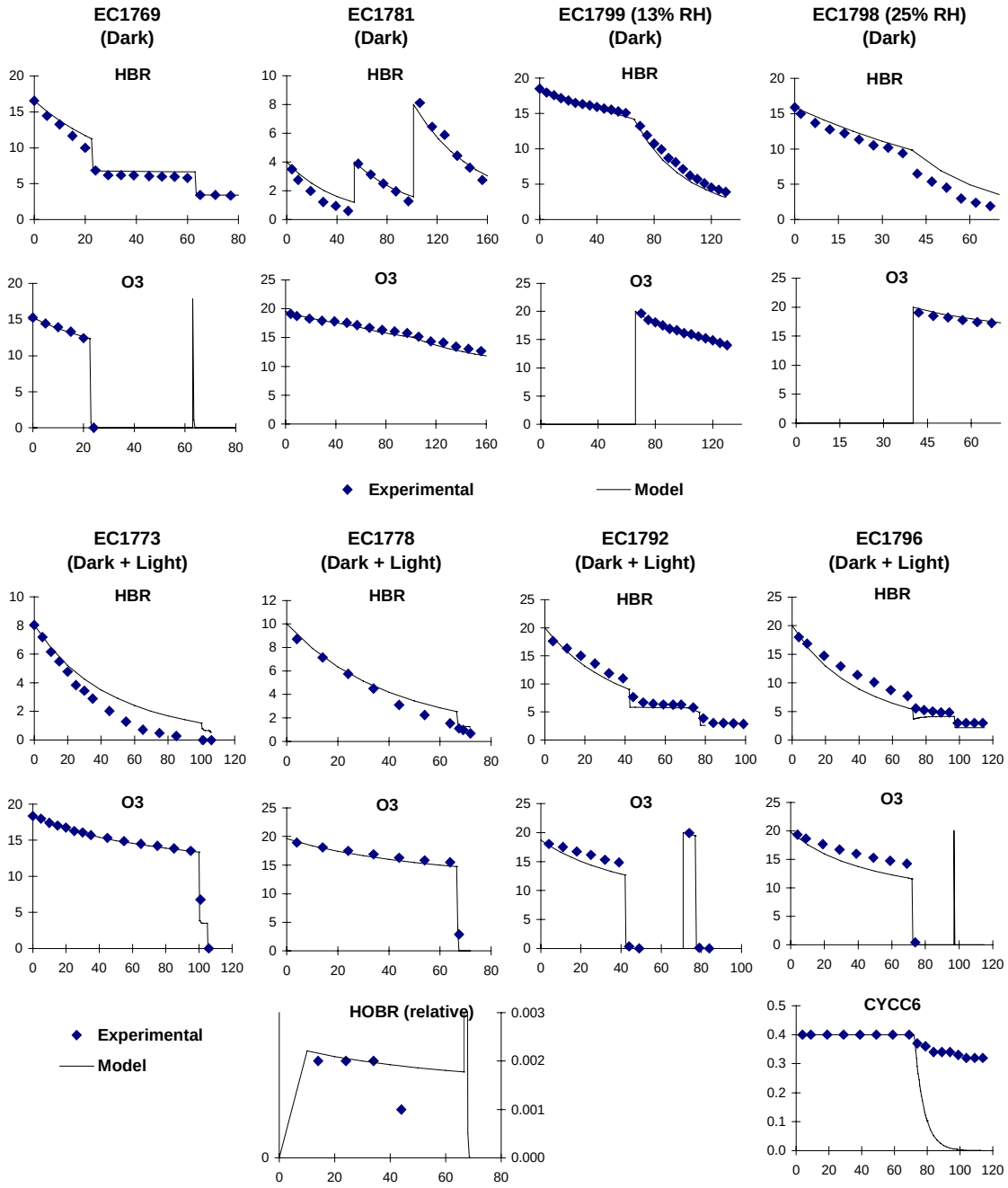

Figure 1. Experimental and calculated concentration-time data for the Ozone + HBr dark and dark + irradiation experiments. The left hand axis on the HOBr plots show the calculated concentrations, the right hand axis on this plot is blank because the absolute experimental concentrations are not known, and the data should be used only to indicate relative concentration trends. Concentrations are in ppm, time is in minutes.

Note that there is no significant net sink for bromine atoms other than formation of highly photoreactive Br_2, so the chain reactions consuming O_3 are extremely rapid. Much less HBr consumption occurs during this process because the reaction of BrO with O_3 is more rapid than its reaction with HBr (see Table 1), and the reaction of OH with Br_2 is calculated to occur at a more rapid rate than its reaction with HBr.

The model correctly predicts that the radical tracer cyclohexane present in run EC1796 reacts when the HBr + O_3 mixture is irradiated, though it significantly overpredicts the amount of reaction occurring. Although the OH radicals are predicted to be formed in this system and the rate constant for the reaction of cyclohexane with OH is almost three orders of magnitude than the probable rate constant for the Br + cyclohexane reaction (see Table 1), the model calculates that the Br levels are sufficiently high that it is the dominant process for cyclohexane consumption. However, the Br + cyclohexane rate constant is very uncertain, and may well be significantly less than the value listed on Table 1. The cyclohexane consumption data are much better fit if it is assumed that this rate constant is a factor of ~20 less than the estimated value on Table 1, though the consumption data are significantly underpredicted if the rate constant is assumed to be much lower than that. Better fits to the cyclohexane consumption data in O_3 + HBr + formaldehyde run EC1797, discussed below, are also obtained if this lower Br + cyclohexane rate constant is assumed.

Alternatively, better fits to the cyclohexane consumption data can also be obtained if there is some unknown sink for Br atoms in these experiments that corresponds to a unimolecular loss rate of ~10^2 min^{-1}. If such a sink exists it must not involve formation of HBr, since otherwise the model would predict that HBr would be regenerated in these HBr + O_3 photolysis experiments, which is not observed. Assuming that this process occurs has no significant effect on model predictions of any other of the experimental measurements carried out during this program.

IR bands attributed to HOBr were observed in runs EC1778 and EC1781, though the amounts were not quantified because of lack of absorption cross section data. No HOBr was detected after the lights were turned on, as is expected due to its rapid photolysis. As shown on Figure 1, this is qualitatively consistent with model predictions.

HBr + O_3 + Formaldehyde Irradiations

The addition of formaldehyde to the HBr + O_3 photolysis system is expected to slow down the rate of loss of O_3 because the reaction of Br with formaldehyde provides a sink for Br. In addition measurements of the rates of consumption of photolysis gives a means to test model predictions of rates of Br atom production in this system. Therefore, several HBr + O_3 + formaldehyde irradiation experiments were carried out. In some experiments the HBr and O_3 were permitted to react in the dark before the lights were turned on to allow Br_2 to build up, and in others the HBr was added after the irradiation began so there would be no time for Br_2 to build up.

Figure 2 shows the results of the experiment where O_3, HBr, and formaldehyde were reacted in the dark, and then the lights were turned on for short (30 second) intervals so the consumption rates would not be too fast to measure. There is no indication of formaldehyde participating in the dark reaction, since its concentration in the dark was relatively stable, and the O_3 and HBr consumption rates are reasonably well fit by predictions of the model that assumes no such formaldehyde involvement. When the lights were turned on, both the O_3 and formaldehyde were consumed, and buildup of CO, expected to be formed when formaldehyde reacts, was observed. As shown on the figure, the model gave a good simulation of the rates of O_3 and formaldehyde consumption and CO formation, though it incorrectly predicted that the HBr consumption continued at approximately the same rate as during the dark reaction.

Figure 3 and Figure 4 show the data from the three experiments where HBr was added during the irradiation of a formaldehyde + O_3 mixture. This procedure was used to investigate the reaction when the buildup of Br_2 due to the dark reaction of HBr and O_3 was minimized. Figure 3 shows the data prior to the HBr addition, and Figure 4 shows the data after the HBr was added. Note that cyclohexane was present as a radical tracer in one of the experiments (EC1797), but otherwise the conditions of all three experiments were similar. Figure 3 shows that the irradiation of O_3 + formaldehyde mixtures causes both O_3 and formaldehyde to be slowly consumed and for CO buildup to occur. Some consumption of the cyclohexane tracer is also observed in the run where it is added, indicating the formation of OH radicals. This is attributed to the photolysis of formaldehyde HO_2 radicals, which then react with O_3 to form OH, as well as by other means.

$$HCHO + h\nu \rightarrow HCO + H \xrightarrow{O_2} 2\ HO_2 + CO$$

$$HO_2 + O_3 \rightarrow OH + 2\ O_2$$

$$HCHO + HO_2 \rightarrow \rightarrow HOCH_2OO\cdot$$

$$HOCH_2OO\cdot \rightarrow HCHO + HO_2$$

However, although the model is qualitatively consistent with these data, it significantly underpredicts the rates of O_3, formaldehyde, and tracer consumption and rates of formation of CO. Higher formaldehyde and tracer consumption rates can be predicted if it is assumed that an additional OH-forming route occurs in the HCHO + HO_2 reaction, but this does not improve the underprediction of the O_3 consumption rates. Increasing the formaldehyde photolysis rate by a factor of ~8 significantly improves the fits to the formaldehyde, CO, and tracer data, though the O_3 consumption rate is still slightly underpredicted. However, since the formaldehyde absorption cross sections and quantum yields are reasonably well established (Atkinson et al, 1997; NASA, 1997) and the light intensity and spectrum is measured in these experiments, it is considered unlikely that this could be the cause of this discrepancy. The reasons for this underprediction of reaction rates in the formaldehyde + O_3 irradiation experiments, which is unrelated to uncertainties in bromine chemistry, is therefore unknown.

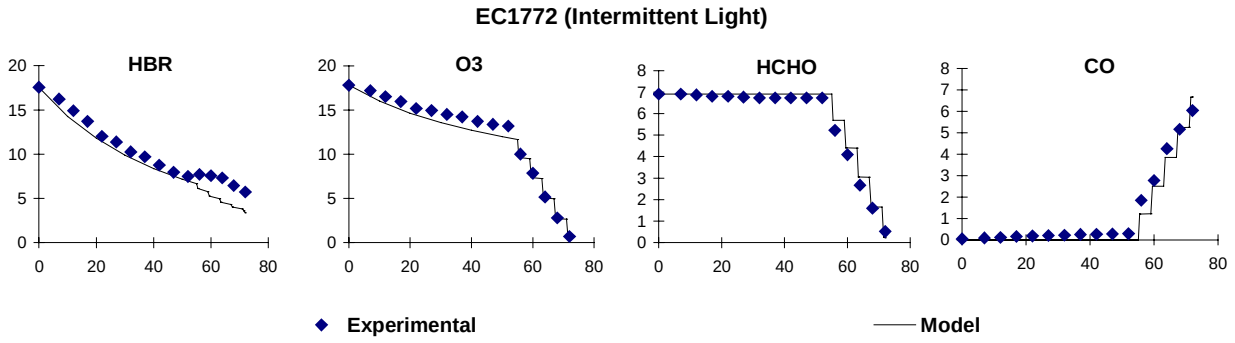

Figure 2. Experimental and calculated concentration-time data for the HBr + ozone + formaldehyde intermittent irradiation experiment. Concentrations are in ppm, time is in minutes.

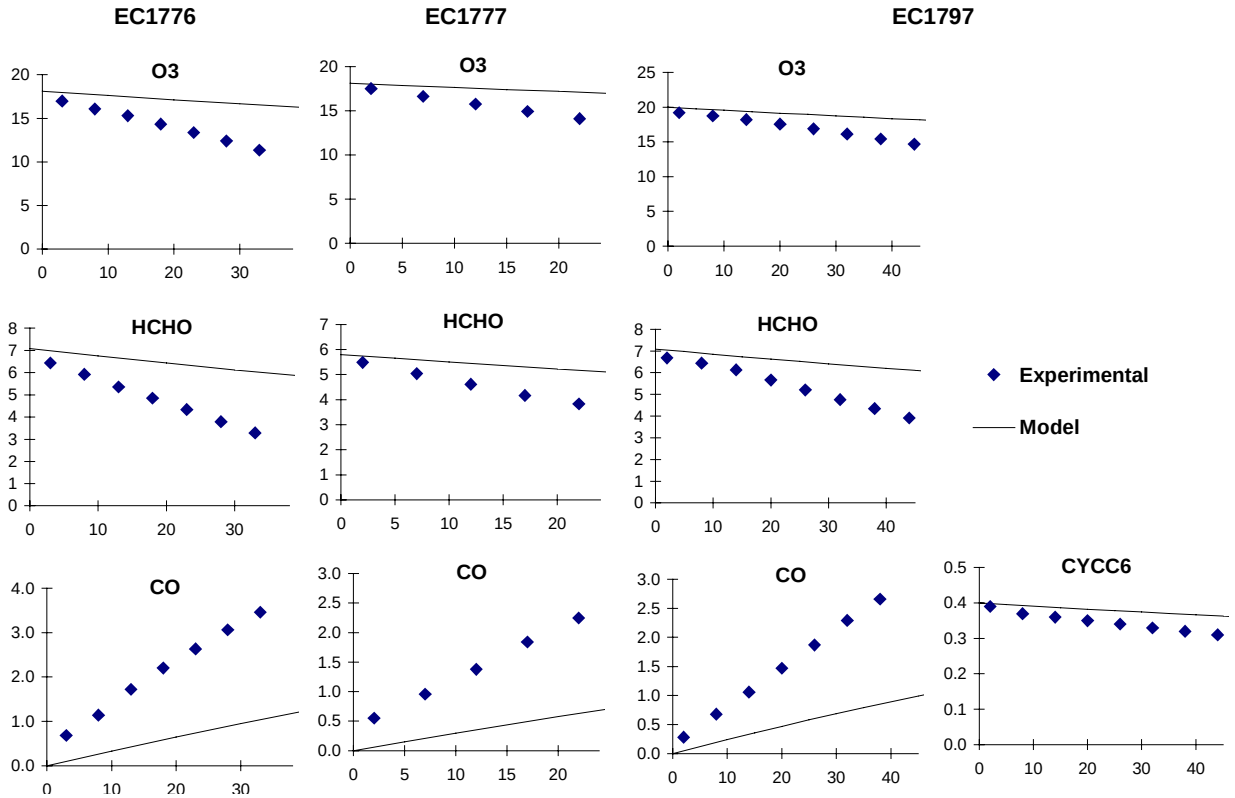

Figure 3. Experimental and calculated concentration-time data for the formaldehyde + ozone irradiation experiments prior to the HBr addition. Concentrations are in ppm, time is in minutes.

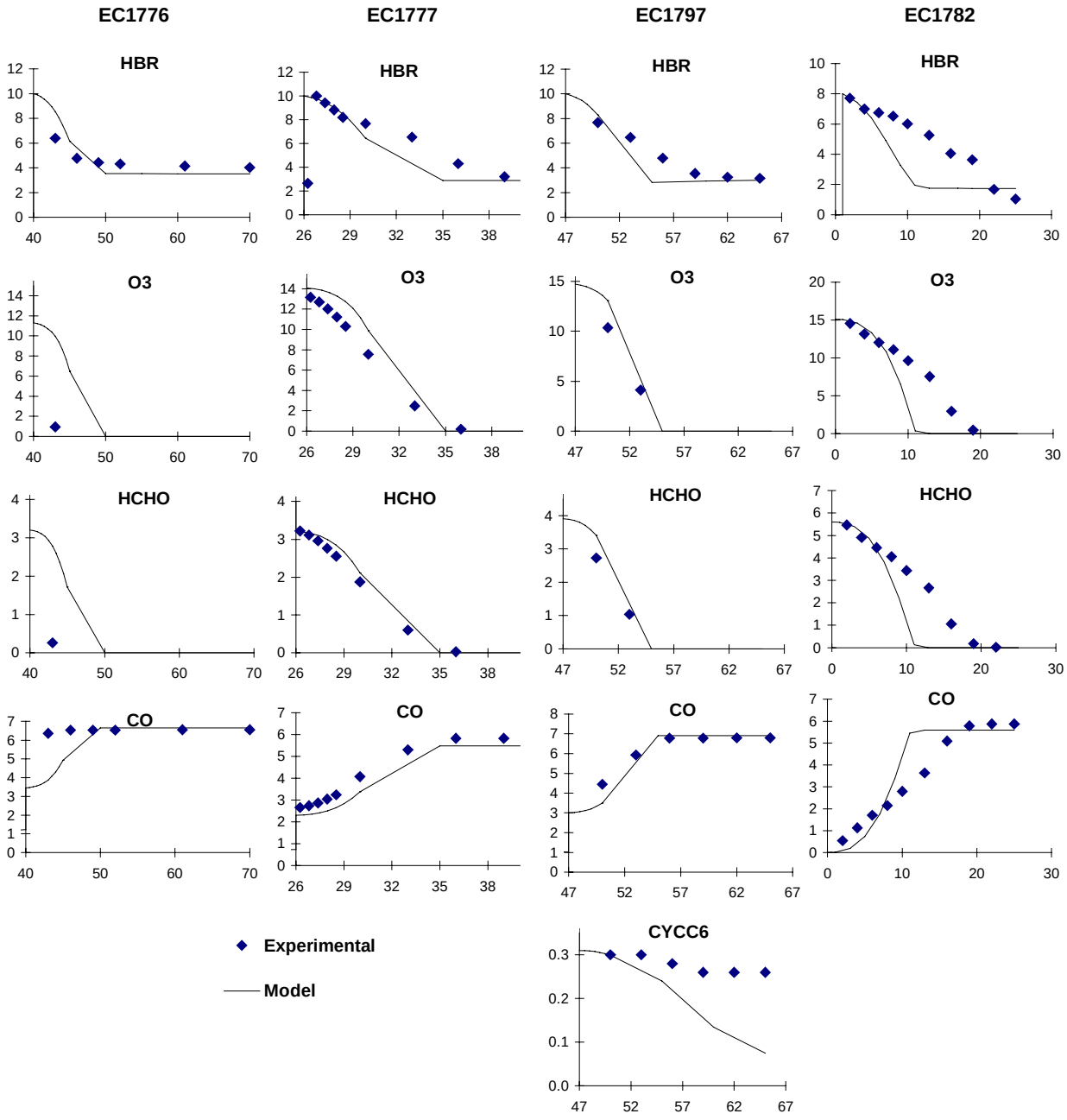

Figure 4. Experimental and calculated concentration-time data for the formaldehyde + ozone irradiation experiments after the HBr addition. Concentrations are in ppm, time is in minutes.

The addition of HBr to the formaldehyde + O_3 irradiation caused the formaldehyde and O_3 to be completely consumed in about 10 minutes or less, and also caused a slight decrease in the radical tracer levels in the run where it is present. The results of EC1776 are somewhat inconsistent with the results of EC1777 and EC1797 in that the consumption rates were more rapid in the first experiment, despite having similar reactant concentrations. The model underpredicted the consumption rates of that first experiment, but gave reasonably good fits to the O_3, formaldehyde and CO data for EC1777 and EC1797. The reason for the discrepancy with run EC1776 is unknown.

The model overpredicted the rate of consumption of the cyclohexane tracer present in run EC1797, though in this case it did not predict it was completely consumed. As indicated above, better fits to these data could be obtained if it is assumed that Br atoms react much with cyclohexane about a factor of 20 times slower than assumed in our mechanism. Alternatively, better fits are also obtained if it is assumed that there is some unknown sink for Br atoms that does not involve re-generation of HBr. The adjustments that fit the tracer data in run EC1796, above, also fit the tracer data in this run.

Figure 4 also shows the data for run EC1782, where the HBr was added only 1 minute after the beginning of the irradiation of the O_3 + formaldehyde mixture. The HBr, O_3, and formaldehyde consumption rates were observed to be somewhat slower than observed in the other experiments, and they were also slower than predicted by the model. In other words, the data suggest that adding the HBr immediately after the beginning of the irradiation of the O_3 + formaldehyde mixture causes a slower rate of reaction than if the HBr is added after the mixture has been irradiated for a longer period. The model does not predict that this should be the case.

Br_2 + Formaldehyde Experiments

In order to further investigate whether the model correctly predicts the photolysis rate of Br_2 and adequately represents the chemistry of the Br + formaldehyde system in the absence of O_3, two experiments were carried out where Br_2 was irradiated in the presence of formaldehyde with no other reactants present. To avoid the reactions occurring at rates too fast to measure, the system was irradiated only for 30 second intervals, with concentration measurements being made between irradiations. The results of these two experiments are shown on Figure 5, which also shows the results of the model calculations. Br_2 is not shown because it could not be measured by the methods available in this study, and its for modeling purposes its initial concentration is calculated based on the known amount of Br_2 injected and the known volume of the chamber.

The irradiations caused formaldehyde to be consumed and HBr and CO to be formed at rates that were in excellent agreement with model predictions. This indicates that the model probably uses approximately the correct Br_2 photolysis rate. On the other hand, formic acid and H_2O_2 are also observed

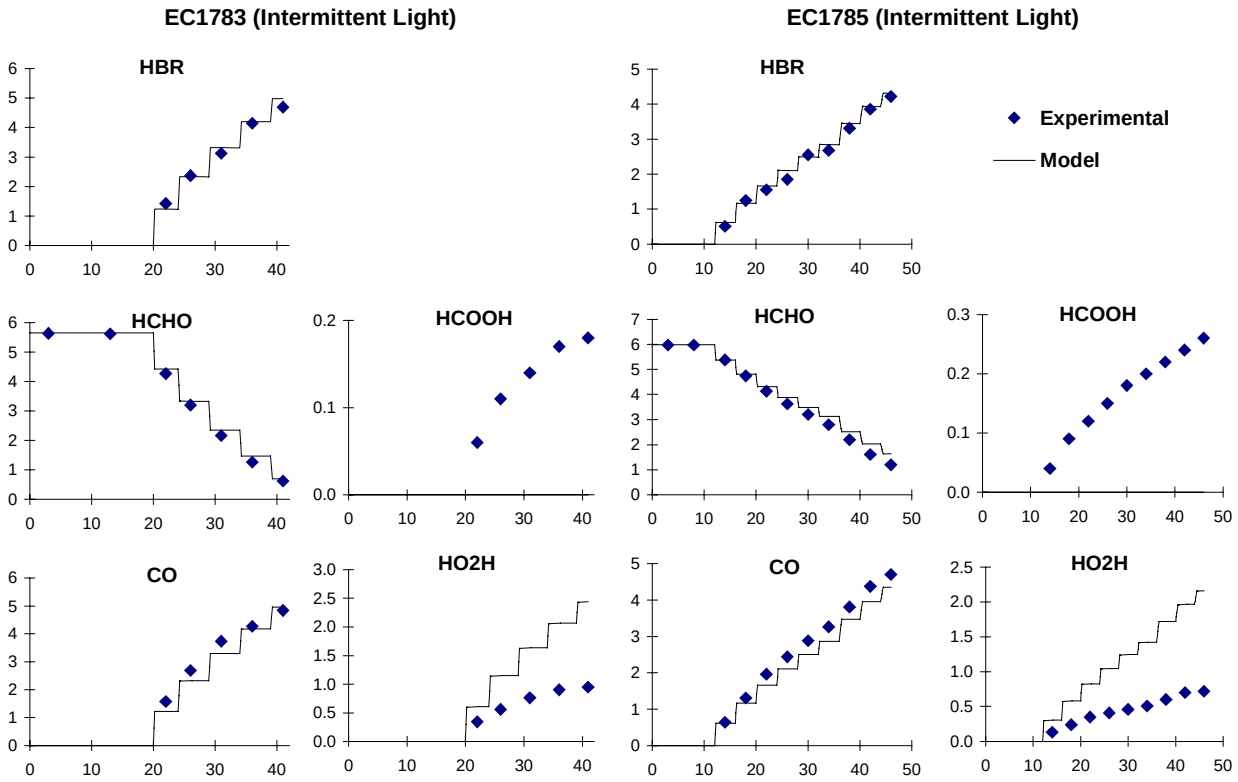

Figure 5. Experimental and calculated concentration-time data for the Br_2 + formaldehyde intermittent irradiation experiments. Concentrations are in ppm, time is in minutes.

to be formed, with the formic acid not being predicted by the model, and the H_2O_2 being formed in yields that are about half of what the model predicts.

The formic acid observed in these experiments can be well simulated if it is assumed that the adduct formed when HO_2 reacts with formaldehyde decomposes approximately 2% of the time to form formic acid and OH, e.g.,

$$HOCH_2OO\cdot \rightarrow OH + HC(O)OH$$

instead of decomposing back to formaldehyde and HO_2. This does not result in any changes to the predictions of H_2O_2 yields, nor does assuming this reaction occurs at this rate have any effect on model simulations of the O_3 + formaldehyde irradiations discussed above.

The reason for the discrepancy between the predicted and experimental H_2O_2 data is not known. The model predicts that formation of H_2O_2 is the major sink for the HO_2 formed when formaldehyde reacts with Br. Assuming H_2O_2 decays to the walls at the same rate as does HBr does not significantly

affect the results. Assuming an HBr + H_2O_2 reaction (presumably forming H_2O and BrOH) results in improved fits for H_2O_2, but only at the expense of significantly underpredicting HBr. Assuming that Br reacts with H_2O_2 at a rapid rate results in an underprediction of the formaldehyde consumption rate, and is also inconsistent with the IUPAC (Atkinson et al, 1997) recommendation that the rate constant for this reaction has an upper limit of 5×10^{-16} cm^3 $molec^{-1}$ s^{-1}. If that upper limit is correct, then the reaction is too slow to be significant in this system.

HBr + NO_x Experiments

Four experiments were carried out where HBr was irradiated in the presence of NO and/or NO_2, and the results of these experiments are shown on Figure 6. In the dark period of HBr + NO experiments there was no significant enhancement of the HBr decay caused by the presence of the NO (see Table 5, above), but NO was converted to NO_2 because of its dark reaction with O_2. As discussed above there was a slight enhancement of the HBr consumption rate in the dark in the presence of NO_2, though this may be a wall reaction. Small amounts of BrNO was formed in both types of experiments, though the amounts could not be quantified. It appears to be a product of slow dark reactions of HBr with both NO and NO_2. Evidence for a reaction of HBr with NO_2 comes from its formation in run EC1779 in the absence of NO, while evidence for its formation from HBr + NO comes from its formation at a higher rate in EC1780, which had lower NO_2 levels than EC1779 but relatively high NO levels. Note that these reactions may be occurring on the walls.

When the lights were turned on the rate of oxidation of NO to NO_2 decreased in the HBr + NO experiments, and there was only a slight increase in the HBr consumption rate. In the HBr + NO_2 experiments the lights caused NO_2 to be converted relatively rapidly to NO, and caused a somewhat greater enhancement in the HBr consumption rate than in the HBr + NO runs.

The model correctly predicted that the reaction rates in the HBr + NO irradiation are relatively slow, and that the NO_2 is converted to NO in the HBr + NO_2 irradiation. However, it predicted that NO was still slowly oxidized to NO_2 in the HBr + NO runs, while experimentally no such oxidation took place, it slightly underpredicted the NO_2 to NO conversion rate in the HBr + NO_2 experiments. The model also underpredicted the HBr consumption rates during the irradiations, particularly in the HBr + NO_2 runs. The model also did not predict that BrNO would be formed in the dark, but predicted that it would be formed in small yields during the irradiations. The concentration predicted to be formed by the end of the irradiations was comparable to the approximate concentrations observed, though as shown on Figure 6, the concentration-time profiles were quite different.

According to the model, the major reactions involving bromine in these experiments are as follows:

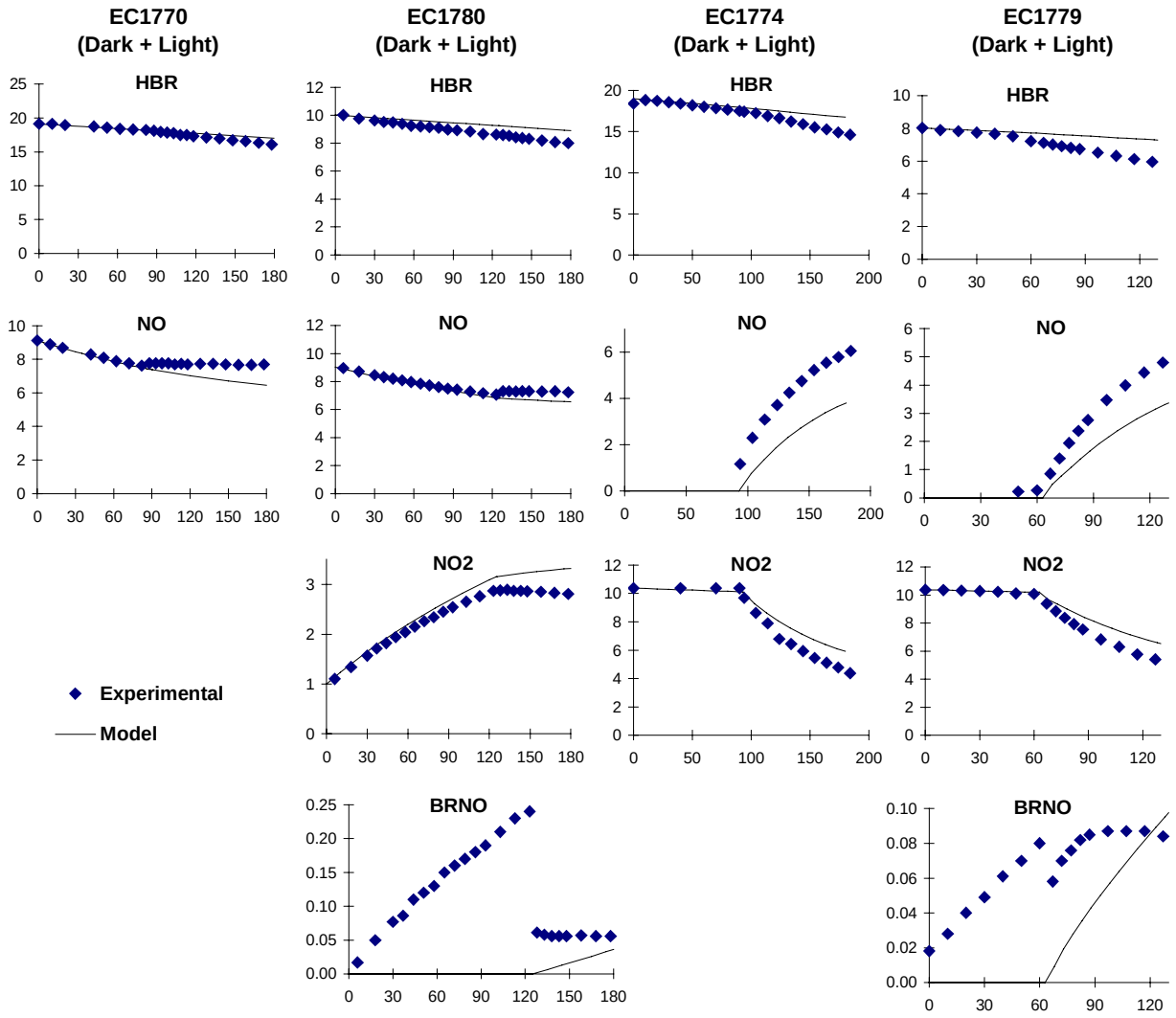

Figure 6. Experimental and calculated concentration-time data for the HBr + NO and HBr + NO_2 dark and irradiation experiments. Concentrations are in ppm, times are in minutes.

$$OH + HBr \rightarrow H_2O + Br \quad (9)$$

$$Br + NO + M \rightarrow BrNO + M \quad (10)$$

$$Br + NO_2 + M \rightarrow BrONO + M \quad (11)$$

$$BrONO + NO \rightarrow BrNO + NO_2 \quad (12)$$

$$BrNO + h\nu \rightarrow Br + NO \quad (13)$$

The OH radicals are formed from the "chamber radical source" (Carter et al, 1982, 1995) which is assumed to be the formation of HONO from NO_2 on the walls, where the HONO subsequently photolyzes to form HONO, and the bromine atoms are introduced into the system primarily by reaction of OH with HBr. The formation from the HBr + O_3 reaction sequence, discussed above, is minor in this system because of the inhibition of O_3 by the relatively high levels of NO. The only significant sink for Bromine in this system is BrNO, which, though it photolyzes rapidly in these experiments (with a calculated photolytic half life of ~1 minute), is also equally rapidly re-formed by the reactions of Br with NO or (after several reactions) with NO_2. The calculated BrNO yields are relatively low in these experiments (see the BrNO plots on Figure 6 for representative values) because the initiation by the chamber radical source is relatively slow.

Note that the conversion of NO_2 to NO observed during the irradiation in the HBr + NO_2 experiments is unrelated to bromine chemistry, since the model predicts almost exactly the same NO and NO_2 profiles in these experiments if HBr is assumed not to be present. This conversion is caused by the reactions

$$NO_2 + h\nu \rightarrow O^3P + NO$$

$$O^3P + NO_2 \rightarrow NO + O_2$$

and the conversion by the Br + NO_x reactions, shown above, is relatively minor. Modifying the magnitude of the chamber radical source assumed in the model calculations only affects the predicted BrNO yields.

The model prediction that the major sink for Br is BrNO and that there is no significant net sink for this compound is inconsistent with the observation that the BrNO levels are approximately constant during the irradiation. Some loss process for BrNO must be occurring if in fact its concentration is increasing due to the generation of Br from OH + HBr.

Br_2 + NO_x Experiments

One experiment each was carried out where Br_2 was irradiated in the presence of NO or NO_2. Because of the rapid photolysis rate of Br_2 the irradiations were carried out intermittently during the first part of the experiments, and then continuously after the changes in reactant and product concentrations

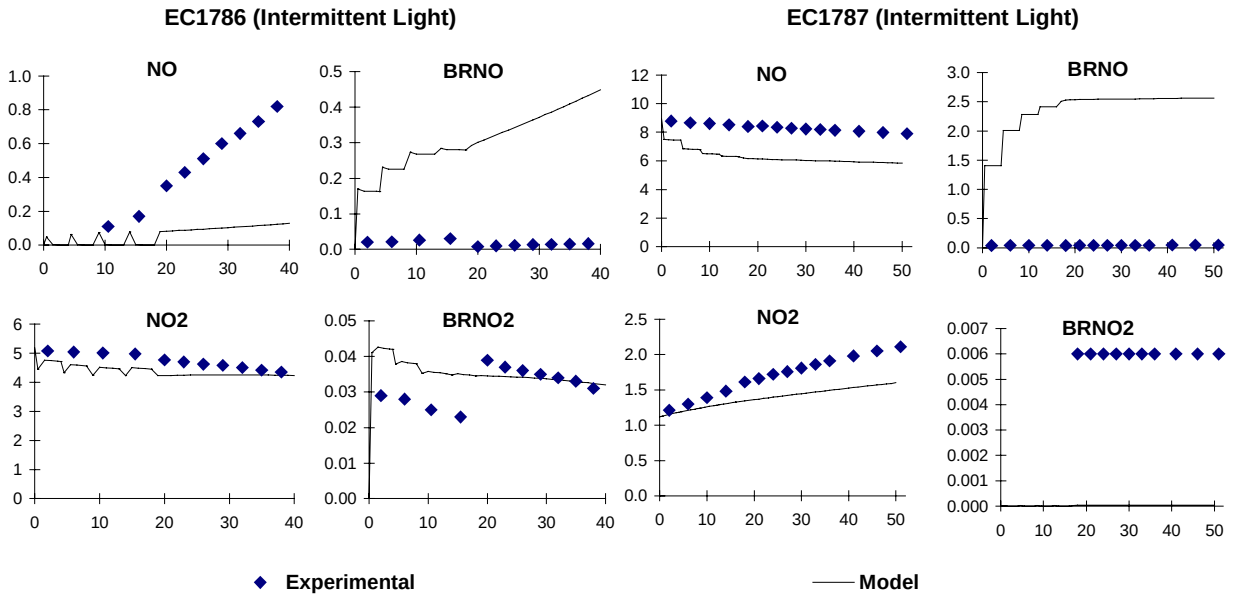

Figure 7. Experimental and calculated concentration-time data for the Br_2 + NO_x intermittent irradiation experiments. Concentrations are in ppm, times are in minutes.

were found to be relatively slow. The data obtained are shown on Figure 7, along with results of model calculations. Conversion of NO to NO_2 was observed in the Br_2 + NO experiment, conversion of NO_2 to NO was observed in the Br_2 + NO_2 run, and formation of low levels of BrNO and $BrNO_2$ were observed in both runs.

Figure 7 shows that the model performs extremely poorly in simulating these experiments, significantly underpredicting the rate of conversion of NO_2 to NO in the Br_2 + NO_2 experiment, and overpredicting, by orders of magnitude, the BrNO yields. As with the HBr + NO_x experiments discussed above, the model predicts that BrNO is the only significant net sink for Br atoms in this system, other than Br_2 itself. Indeed, because there is no unreactive net sink for Br atoms in this system, the model predicts that there is relatively little net consumption of Br_2, and the net consumption that does occur is manifested by the formation of BrNO.

Various attempts were made to determine which reasonable modifications to the mechanism or possible additional reactions might be added that might improve the ability of the model to simulate the results of the HBr and Br_2 + NO_x experiments. No reasonable adjustments or added reactions were found to improve the performance of the model in simulating these experiments. The most reasonable loss processes BrNO all involve the formation of Br_2 or Br, which results in no net sink for Br and therefore BrNO and Br_2. Assuming a hydrolysis of BrNO to HBr and HONO at a significant does not solve the

problem because (1) such a reaction is estimated to be ~10 kcal/mole endothermic and the H_2O concentrations are very low in these experiments and (2) it does not result in significant improvements of model simulations of the NO and NO_2 profiles. Assuming an unknown Br atom sink at the rate that fits the radical tracer data in the HBr + O_3 irradiations does not significantly affect any of the measured species in these HBr and Br_2 + NO_x experiments. Other alternatives of various degrees of chemical reasonableness were examined, without any significant success.

HBr + NO_x + Formaldehyde and Br_2 + NO_x + Formaldehyde Experiments

The HBr + NO_x and Br_2 + NO_x experiments discussed above do not represent a particularly realistic approximation of ambient conditions because under ambient conditions there would be sufficient sinks for Br atoms that highly photoreactive species such as Br_2 and BrNO would not be predicted to build up in concentration. To provide a somewhat more realistic representation in this regard, a HBr + NO_2 and a Br_2 + NO_2 experiment was carried out with formaldehyde added to serves as a sink for Br atoms. The results of the HBr + NO_2 + formaldehyde experiment is shown on Figure 8 and those for the Br_2 + NO_2 + formaldehyde run are shown on Figure 9. Results of model simulations of these experiments are also shown. Note that the irradiation was continuous for the experiment with HBr but was intermittent for the run with Br_2 in order to obtain measurable reaction rates. N-heptane was present as a radical tracer in the Br_2 + NO_2 + formaldehyde experiment.

In the HBr + NO_2 + formaldehyde run, there was no apparent reaction after the compounds were mixed in the dark, except for a slightly enhanced rate of HBr decay, as was observed in the HBr + NO_2 experiment. In this case, however, no BrNO was observed in the IR analysis. Turning on the lights caused the NO_2 to be converted to NO and the formaldehyde to be oxidized to CO, with the formaldehyde being completely oxidized in about 80 minutes.

In the Br_2 + NO_2 + formaldehyde experiment, the intermittent irradiations caused formaldehyde and NO_2 to be consumed (though more of the former than the latter), and formation of CO, formic acid, and a number of nitrogen-containing products to be observed. These included, in approximate order of maximum yield, HNO_3, HO_2NO_2, HONO, N_2O_5, $BrNO_2$ and BrNO. Approximately 1 ppm of HBr was observed after the end of the second irradiation, but it was not observed to increase further in subsequent irradiations. A very small amount (~5%) of the n-heptane radical tracer was consumed after the four irradiations.

The model did not perform particularly well these experiments. In the HBr + NO_2 + formaldehyde run, significantly underpredicting the formaldehyde consumption and CO formation rate, though giving somewhat better simulations of the NO_2 to NO conversion rate. The model simulation without the HBr added predicts a slightly faster NO_2 to NO conversion rate and approximately half of the consumption of the formaldehyde that is predicted with the HBr present.

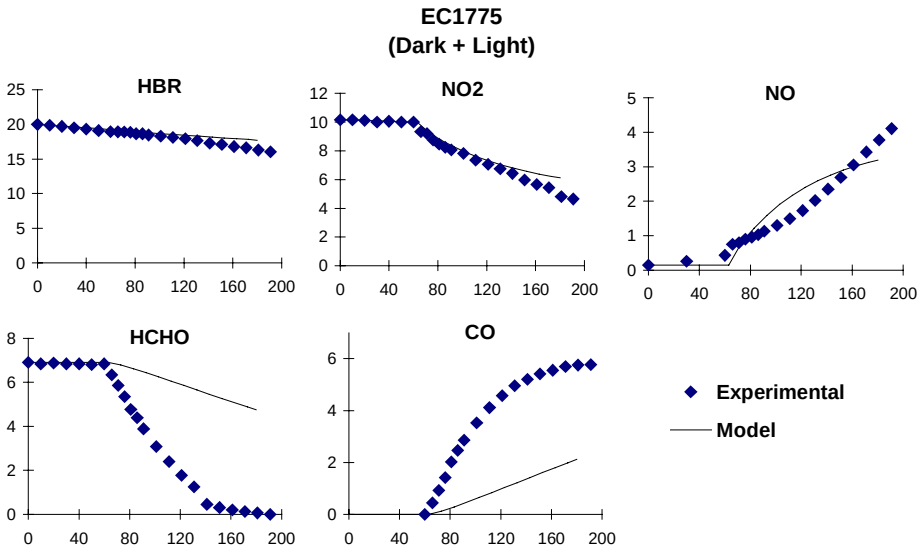

Figure 8. Experimental and calculated concentration-time data for the HBr + NO_2 + Formaldehyde dark and irradiation experiment. Concentrations are in ppm, times are in minutes.

The significant underprediction of the effect of HBr on the formaldehyde consumption rate suggests that the model is underpredicting the rate of Br atom formation in this experiment. According to the model, the major source of Br atoms in this experiment is the reaction of OH with HBr, with the OH coming primarily from the reaction of NO with the HO_2 formed from the photolysis of formaldehyde. Increasing the photolysis rate of formaldehyde photolysis by the same factor that improves the fits to the data in the O_3 + formaldehyde irradiations results in improved fits to the formaldehyde and CO data, but causes the model to significantly underpredict the NO_2 to NO conversion rate. Increasing Br input by increasing the O^3P + HBr rate constant to above its literature value (see Table 1) has a similar effect on the model predictions. The model predicts that the reaction of O_3 with HBr is only a minor source of Br atoms because the O_3 is inhibited by the relatively high concentrations of NO that are present.

The model performance in simulating the Br_2 + NO_2 + formaldehyde run shown on Figure 9 is better in some respects than its performance in simulating the run with HBr, but is still not entirely satisfactory. Considering the uncertainties in the system and the poor performance in simulating the other experiments, the model predicts reasonably well the rates of consumption of formaldehyde and NO_2, and the concentration-time profile for N_2O_5. The latter is predicted to be formed from the reaction of O_3 (formed from the photolysis of NO_2) with NO_2 forming NO_3, which then reacts further with NO_2 to form N_2O_5. The peroxynitric acid (HO_2NO_2) is predicted to be formed from the reactions of HO_2 (formed primarily from the reaction of Br with formaldehyde) with NO_2, and is predicted to thermally decompose rapidly back to HO_2 and NO_2. The overprediction of HO_2NO_2 by the model may be due to an overprediction of HO_2 levels, but it could also be due to the temperature in the experiment being

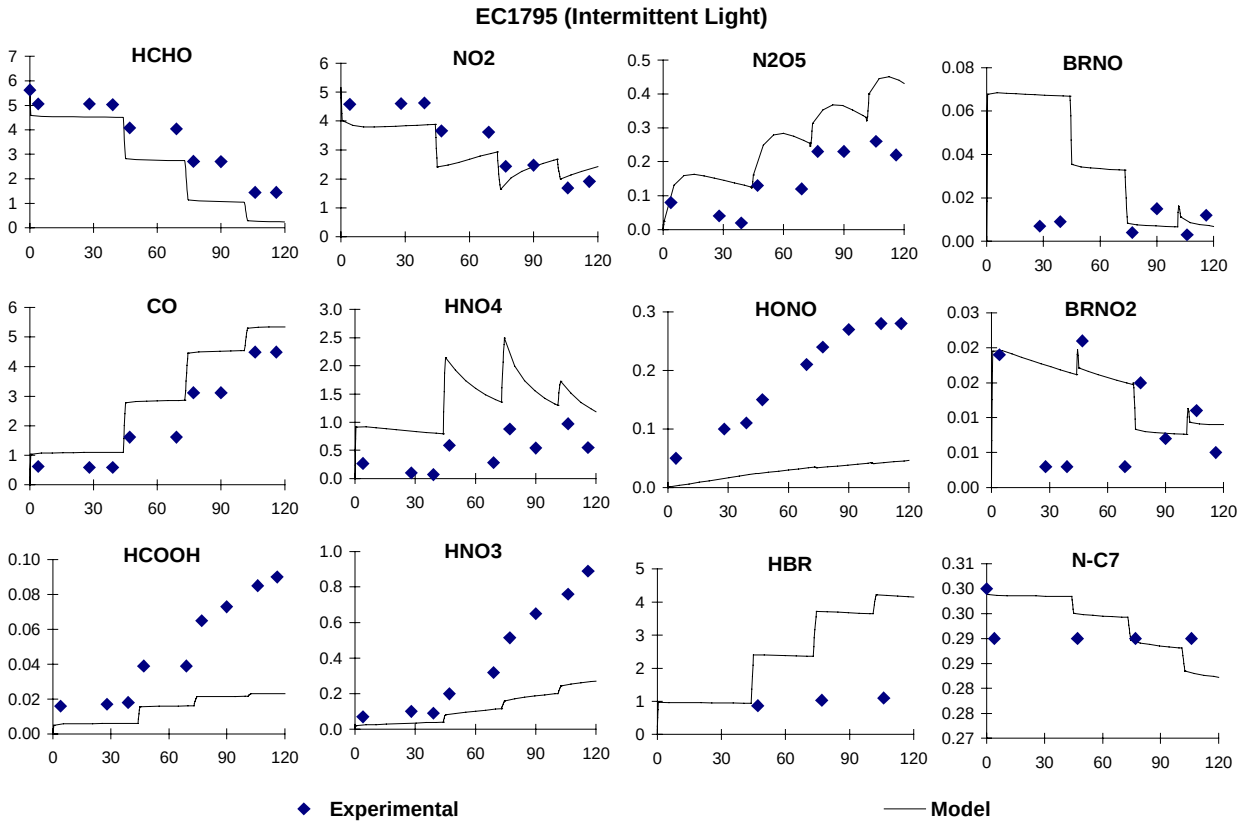

Figure 9. Experimental and calculated concentration-time data for the Br_2 + formaldehyde + NO_x intermittent irradiation experiment. Concentrations are in ppm, times are in minutes.

somewhat higher than represented in the model, since the decomposition of HO_2NO_2 is highly temperature sensitive. The model significantly underpredicts the formation of HONO and HNO_3, which are predicted to be formed from the reactions of OH with NO and NO_2. It may be that there are some processes converting HO_2 to OH or HO_2NO_2 to HONO or HNO_3 that are not being adequately represented by this model. The model correctly predicts that only small amounts of the n-heptane tracer is consumed in this experiment.

The model performance in simulating the formation of bromine-containing species in the Br_2 - NO_2 - formaldehyde run is not satisfactory. The HBr concentrations are significantly overpredicted after the time of the second irradiation, and the BrNO is also overpredicted, though not to nearly as great an extent as it is in the simulations of the runs without formaldehyde. The model does predict approximately the correct magnitude of the $BrNO_2$ concentrations, though it does not simulate how its concentrations vary with time during the intermittent irradiations. No reasonable adjustments to the mechanism result in any improved fits in any of these respects.

Modeling Propyl Bromide Reactivity Experiments with the Revised Mechanism

As discussed above, the re-evaluation of the literature and the results of the experiments in this work resulted in significant changes to our estimated mechanism for the reactions of BrO_x compared to the version used in our previous study of propyl bromide reactivity (Carter et al, 1997). In particular, the rate constant for the HBr + O_3 reaction, which had to be added to the mechanism to fit the propyl and butyl bromide reactivity data, had to be reduced significantly based on the results of this work. In addition, the mechanism for this reaction was also changed to involve the formation of Br_2, which was not used in the previous mechanism. Therefore, the model simulations of the alkyl bromide reactivity experiments given by Carter et al (1997) are not consistent with the results of this study.

Because of this, the propyl bromide reactivity experiments from the study of Carter et al (1997) were re-modeled using the mechanism for the bromine species given in Table 1. The reactions of propyl bromide was exactly the same as derived by Carter et al (1997), except that the bromopropionaldehyde is represented by the lumped higher aldehyde model species rather than using a separate model species that has a very similar mechanism. The base mechanism and the mechanisms of the VOCs in the base case experiments were also updated to the current SAPRC-99 mechanism; Carter et al (1997) used the earlier, SAPRC-97 version.

Figure 10 through Figure 12 show results of model simulations of one each of the three types of the incremental reactivity experiments. The results of the other examples of the three types of experiments were very similar to those that are shown. The model calculations using the mechanism developed in this work are shown with the solid lines on the figures. The figures also show the model simulations using the "placeholder" mechanism for propyl bromide that was used in the version of the SAPRC-99 mechanism given by Carter (2000). This "placeholder" mechanism does not incorporate any attempt to represent bromine chemistry, but instead uses more reactive organic product model species to represent the enhanced reactivity caused by the bromine reactions (Carter, 2000). It is represented by the dashed lines on these figures.

The data on these figures show that the updated mechanism performs very poorly in simulating the propyl bromide reactivity results. As with the "unadjusted" mechanism of Carter et al (1997), the model significantly underpredicts the reactivity of propyl bromide under high NO_x conditions, and fails to predict its inhibiting characteristics under conditions where NO_x is limited. No reasonable mechanisms could be found to improve these fits that are chemically reasonable and consistent with the results of these experiments. Indeed, the highly simplified "placeholder" mechanism for propyl bromide performs significantly better in simulating the reactivity of propyl bromide under high NO_x conditions, though it also does not correctly simulate the inhibition under low NO_x conditions. However, because it does not represent the actual chemistry that is occurring in this system, use of that mechanism for atmospheric reactivity calculations is not recommended.

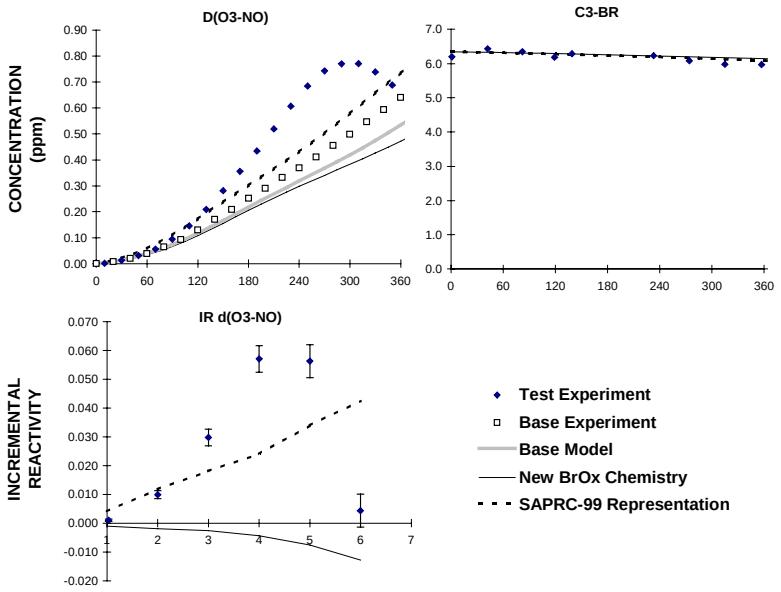

Figure 10. Plots of selected experimental and calculated results of the mini-surrogate + 5 ppm propyl bromide run DTC-421.

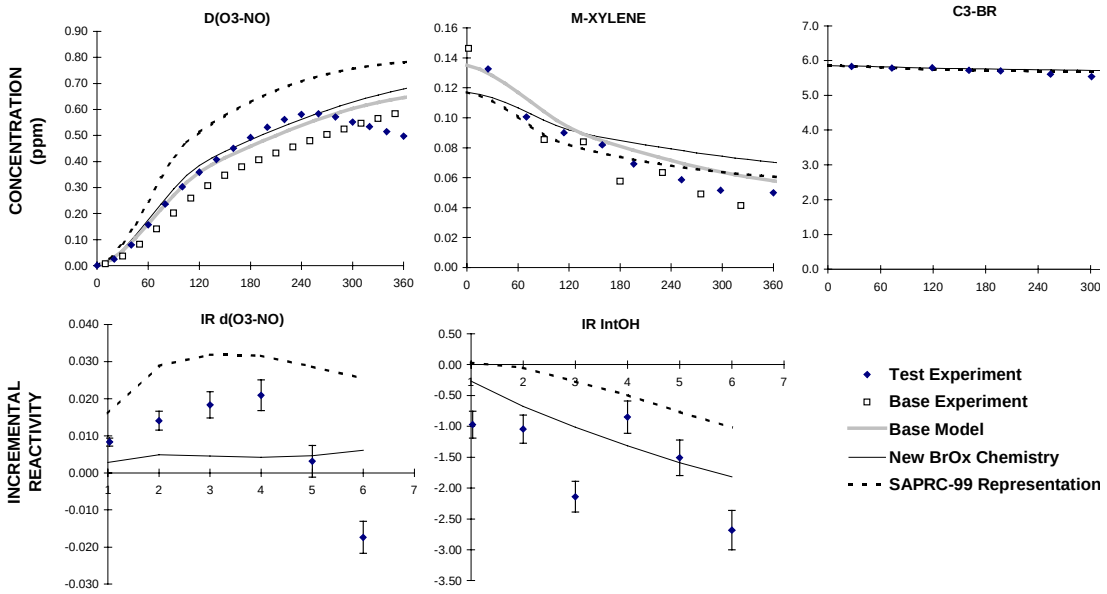

Figure 11. Plots of selected experimental and calculated results of the high NO_x full surrogate + 5 ppm propyl bromide run DTC-427.

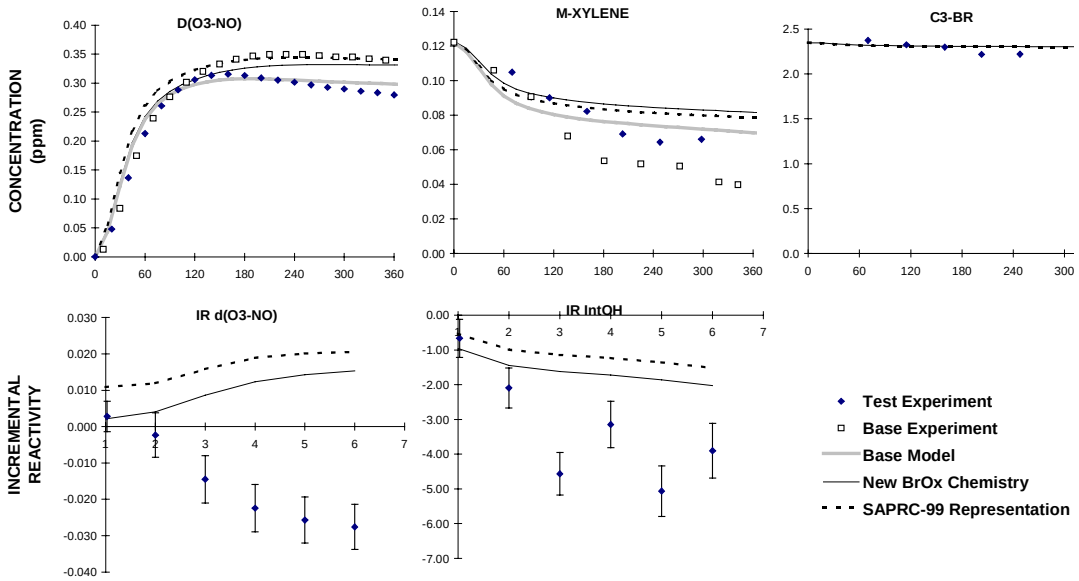

Figure 12. Plots of selected experimental and calculated results of the low NO_x full surrogate + 2 ppm propyl bromide run DTC-424.

CONCLUSIONS

The objective of this program was to obtain data necessary to the development and evaluation of fundamental chemical mechanisms for the reactions of simple bromine-containing compounds under atmospheric conditions. This information is necessary if we are ever to obtain the capability to reliably predict the atmospheric impact of bromine-containing solvents such as propyl bromide. Without this capability, it will not be possible to reliably assess whether this or any other bromine containing compounds may have a negligible impact on ozone formation on the basis of model predictions of its ozone reactivity. Although this project has provided useful information concerning the reactions of simple bromine-containing species such as HBr or bromine atoms under simulated atmospheric conditions, it has also shown that there is much we still do not understand about the atmospheric behavior of such species, particularly in the presence of NO_x. It is concluded that more research is required before we can predictively model the atmospheric reactions of bromine-containing compounds such as propyl bromide.

This program has provided new information concerning the reactions of HBr with ozone under atmospheric conditions, and has shown that the speculative mechanism proposed in our previous attempts to model alkyl bromide smog chamber experiments (Carter et al, 1997) is almost certainly incorrect. The reaction was found to occur at a rate constant which is approximately 10^3 times slower than used by Carter et al, 1997), and also via a different mechanism. In particular, the data indicated that at least two moles of HBr are consumed for each mole of O_3 reacted, which can only be explained if the HOBr formed in the initial O_3 + HBr reaction rapidly reacts with HBr to form Br_2. Although Br_2 was not observed directly in this study, its formation is indicated by the very rapid consumption of O_3 that occurs when the lights are turned on after HBr and O_3 have reacted in the dark, and by the fact that formaldehyde, which reacts with the Br atoms formed when Br_2 photolyzes, slowed down the rate of this consumption. Although HOBr has been known to react with HBr to form Br_2 on ice surfaces, this is the first indication that it may be an important process in simulated photochemical smog systems.

It still uncertain, however, whether the apparent O_3 + HBr and HBr + HOBr reactions are entirely gas-phase processes under the conditions of our experiments, or whether wall reactions may play a role. Indications for possible wall reactions come from the relatively rapid dark wall loss for HBr in this chamber, the fact that the HOBr and HBr reaction is believed to occur on surfaces at least at ice temperatures, and the fact that the apparent O_3 + HBr rate constant determined in this study, though orders of magnitude slower than proposed by Carter et al (1997), is still higher by a factor of ~15 than an upper limit reported by Mellouki et al (1994). On the other hand, the apparent O_3 + HBr rate constant was found to be essentially the same when the chamber was humidified, despite the fact that humidification caused factors of ~5 and ~20 increases in the HBr wall loss rates. If this reaction were primarily a wall-mediated process, then one would expect it to be significantly affected by humidity.

Note that if the O_3 + HBr reactions were wall mediated, one would expect that these reactions should be slower in the alkyl bromide reactivity experiments of Carter et al (1997) than they were in the chamber used in this study. By all known measures the surfaces of the FEP Teflon film chambers used by Carter et al (1997) tend to be less reactive than the quartz and Teflon-coated metal surfaces present in the EC chamber used in this work. (See, for example, the discussion of chamber wall effects by Carter et al, 1995, and references therein.) Therefore, it is not credible to invoke surface processes as the sole rationalization to justify modeling the Carter et al (1997) experiments using O_3 + HBr rate constants that are 10^3 times higher than are consistent with the data obtained in this work.

The use of formaldehyde to evaluate the role of Br atoms in our experiments turned out to be complicated by the fact that the base mechanism apparently does not adequately represent some aspects of the formaldehyde reactions under the conditions of these experiments. Higher rates of formaldehyde and O_3 consumption were observed when O_3 and formaldehyde were photolyzed than predicted by the mechanism, and higher than predicted yields of formic acid were observed as a formaldehyde oxidation product. The formic acid could be successfully simulated in almost all cases if it is assumed that its formation is a minor (~2%) product of the HO_2 + formaldehyde reactions. On the other hand, the high rate of reactions in the formaldehyde + O_3 photolysis system could not be successfully simulated with reasonable modifications to the mechanism. This lead to some uncertainties in evaluating causes for failures of model simulations in experiments involving HBr, but is probably less of a factor in evaluations of experiments involving Br_2 because of the relatively slow rates of these reactions compared to Br_2 photolysis.

Although there are some discrepancies that may involve problems with our representation of formaldehyde chemistry, it appears likely that the bromine reactions in the absence of NO_x are relatively straightforward and may be reasonably well represented by the present model. Uncertainties exist concerning the fate of Br in experiments where there is no known sink for Br other than the formation of highly photoreactive Br_2, where the high levels of Br atoms may be reacting with trace impurities or on the chamber walls. However, these types of conditions are unlikely to be important in the ambient atmosphere.

The results of the experiments where bromine species react in the presence of NO_x indicate a much more complex chemical system that is clearly not adequately represented in the present model. The model predicts that BrNO and probably $BrNO_2$ and BrONO are playing an important role, and indeed formation of BrNO and $BrNO_2$ was observed in these experiments. The model does not represent these processes particularly well, incorrectly predicting that BrNO builds up in relatively high concentrations under conditions where there is no known unreactive sink for Br atoms, and incorrectly predicting the effects of Br_2 photolysis on NO and NO_2 interconversion rates. It appears likely that either there are some unknown reaction routes in the Br + NO_2 system that do not involve the formation of BrNO or Br_2, or that there is some unknown sink for BrNO that does not readily regenerate Br atoms. Despite extensive

investigation of possible reactions, we were unable to come up with chemically reasonable or thermodynamically feasible mechanisms to resolve these discrepancies.

The current mechanism is also unable to successfully model the alkyl bromide reactivity experiments carried out in the previous study of Carter et al (1997) without making the assumptions about the rate of the O_3 + HBr reaction that are clearly inconsistent with the results of this study. The additional reactions added to the model to represent the role of Br_2 and the $BrNO_x$ species were not sufficient to improve model performance. Given our inability to understand and successfully model the presumably chemically simpler HBr + NO_x and Br_2 + NO_x experiments carried out in this study, we conclude that we are currently unable to predictively model the atmospheric reactions of propyl bromide or other compounds whose reactions introduce bromine atoms into the atmosphere.

Clearly, additional fundamental research is needed concerning the reactions of bromine atoms and simple bromine-containing compounds in the atmosphere before we can hope to predictively model the ozone formation potential and other atmospheric impacts of bromine-containing compounds. This will include fundamental laboratory studies of compounds such as BrNO and $BrNO_2$, including not only their reactions with the various types of compounds and radicals that are present in the atmosphere, but also their reactions on various types of surfaces. In addition, the question of whether surface processes are important in the HBr + O_3 system can only be resolved by studying these reactions on a variety of types of surfaces. Unfortunately, the present study has tended to raise more questions than it answered, and unless there is an unanticipated breakthrough that resolves these questions it will probably take considerable research before we can successfully model these highly complex systems.

REFERENCES

Abbatt, J. P. D. (1994): Geophys. Res. Lett. 21, 665-668.

Atkinson, R., D. L. Baulch, R. A. Cox, R. F. Hampson, Jr., J. A. Kerr, M. J. Rossi, and J. Troe (1997): "Evaluated Kinetic, Photochemical and Heterogeneous Data for Atmospheric Chemistry: Supplement V and VI, IUPAC Subcommittee on Gas Kinetic Data Evaluation for Atmospheric Chemistry," Phys. Chem. Ref. Data, 26-, 521-1011 (Supplement V) and 1329-1499 (Supplement VI).

Barnes, I.; Bastian, V.; Becker, K.H.; Overath, R.; Tong, Z. (1989): "Rate constants for the reactions of Br atoms with a series of alkanes, alkenes, and alkynes in the presence of O2," Int. J. Chem. Kinet. 21, 499.

Baulch, D.L.; Duxbury, J.; Grant, S.J.; Montague, D.C. (1981): "Evaluated kinetic data for high temperature reactions. Volume 4 Homogeneous gas phase reactions of halogen- and cyanide-containing species," J. Phys. Chem. Ref. Data 10, Supplement.

Bierbach, A., I Barnes, and K. H. Becker (1996): "Rate Coefficients for the Gas-Phase Reactions of Bromine Radicals with a Series of Alkanes, Alkenes, Dienes, and Aromatic Hydrocarbons at 298±2 K," Int. J. Chem. Kinet. 28, 565-577.

Broeske, R. and F. Zabel (1998): "Kinetics of the Gas-Phase Reaction of BrNO2 with NO," J. Phys. Chem A 102, 8629-8631.

Calvert, J. G., and J. N. Pitts, Jr. (1966): "Photochemistry," John Wiley and Sons, New York.

Carter, W. P. L. (2000): "Documentation of the SAPRC-99 Chemical Mechanism for VOC Reactivity Assessment," Report to the California Air Resources Board, Contracts 92-329 and 95-308, May 8.

Carter, W. P. L., R. Atkinson, A. M. Winer, and J. N. Pitts, Jr. (1982): "Experimental Investigation of Chamber-Dependent Radical Sources," Int. J. Chem. Kinet., 14, 1071.

Carter, W. P. L., D. Luo, I. L. Malkina, and D. Fitz (1995): "The University of California, Riverside Environmental Chamber Data Base for Evaluating Oxidant Mechanism. Indoor Chamber Experiments through 1993," Report submitted to the U. S. Environmental Protection Agency, EPA/AREAL, Research Triangle Park, NC., March 20..

Carter, W. P. L., D. Luo, and I. L. Malkina (1997): "Investigation of the Atmospheric Ozone Formation Potential of Selected Alkyl Bromides," Report to Albemarle Corporation, November 10.

Dimitriades, B. (1999): "Scientific Basis of an Improved EPA Policy on Control of Organic Emissions for Ambient Ozone Reduction," J. Air & Waste Manage. Assoc. 49, 831-838

Dolson,D.A.; Klingshirn,M.D. (1993): "Laser-initiated chemical chain reactions: termination kinetics of the Cl2/HBr/NO chain system", J. Phys. Chem. 97, 6645-6649.

Ferguson, K. C, E. Whittle (1971): “Kinetics of the vapour-phase bromination of cyclanes and n-butane. C-H bond dissociation energies in cyclanes,” Trans. Faraday Soc. 67, 2618.

Frenzel, A; Scheer, V.; Behnke, W.; Zetzsch, C. (1996): “Synthesis and mid-IR absorption cross sections of $BrNO_2$”, J. Phys. Chem. 100, 16447-16450.

Harwood, M. H. , J. B. Burkholder, A. R. Ravishankara (1998): “Photodissociation of $BrONO_2$ and N_2O_5: quantum yields for NO_3 production at 248, 308, and 352.5 nm,” J. Phys. Chem. A: 102, 1309-1317.

Loock, H-P, and C. X. W. Qian (1998): “Photodissociation Studies of Notrosyl Bromide: I. Photofragment Spectroscopy and Electronic Structure,” J. Chem. Phys. 8, 3178-3186.

Mellouki, A., R. K. Talukdar, and C. J. Howard (1994): “Kinetics of the reactions of HBr with O3 and HO_2: the yield of HBr from HO_2 + BrO,” J. Geophys. Res. 99, 22949-2295.

NASA (1997): “Chemical Kinetics and Photochemical Data for Use in Stratospheric Modeling, Evaluation Number 12,” JPL Publication 97-4, Jet Propulsion Laboratory, Pasadena, California, January.

NASA (2000): “Chemical Kinetics and Photochemical Data for Use in Stratospheric Modeling. Supplement to Evaluation 12: Update of Key Reactions. Evaluation Number 13,” JPL Publication 00-3, March 9.

Orlando,J.J. and Tyndall,G.S. (1996): “Rate coefficients for the thermal decomposition of BrONO2 and the heat of formation of BrONO2,” J. Phys. Chem. 100, 19398-1940

Seakins, P .W.; M. J. Pilling, J. T. Niiranen,, D. Gutman, and L. N. Krasnoperov: (1992): “Kinetics and thermochemistry of R + HBr = RH + Br reactions: determinations of the heat of formation of C2H5, i-C3H7, sec-C4H9, and t-C4H9,” J. Phys. Chem. 96, 9847-9855.

Schonle, H. D. Knauth, R. N. Schindler (1979): J. Phys. Chem, 83, 3297.

Turnipseed A. A.; J. W. Birks and G. G. Calvert (1991): “Kinetics and temperature dependence of the BrO + ClO reaction,” J. Phys. Chem. 95, 4356-4364

Wallington, T .J.; L. M. Skewes, W. O. Siegl, and S. M. Japar: (1989): “A relative rate study of the reaction of bromine atoms with a variety of organic compounds at 295K, “Int. J. Chem. Kinet. 21, 1069.

APPENDIX A. DATA TABULATIONS

Table A- 1. Tabulated data for run EC-1767: HBr in Dry Air

Calculated Initial HBr Concentration = 20.0 ppm

	t (min)	Rel. Conc.
Dark Decay →	0	1.0000
	10	0.9900
	20	0.9802
	30	0.9753
	40	0.9705
	50	0.9656
	60	0.9561
	70	0.9513
	80	0.9513
Started Irradn →	83	
6 min from start of irradn →	0	1.0000
	10	0.9950
	20	0.9851
	30	0.9753
	40	0.9705
	50	0.9656
	60	0.9608
	70	0.9513
	80	0.9466
	90	0.9419

Table A- 2. Tabulated data for run EC-1768. HBr + O_3 with Irradiation

Initial HBr = 20.0 ppm

	t (min)	HBr Rel. Conc.	HBr (ppm)	O_3 (ppm)
Dark Decay →	0	1.0000		
	10	0.9900		
	20	0.9802		
	30	0.9753		
	40	0.9705		
	50	0.9656		
	60	0.9656		
	70	0.9608		
	80	0.9561		
	90	0.9561		
	100	0.9561		
	110	0.9513		
Added 17.8 ppm O_3 →	117			
	120	0.8314	16.63	14.49
	130		12.58	12.66
	140		9.56	11.46
	150		7.75	10.69
	160		5.61	9.87
	170		4.22	9.34
	180		2.90	8.80
	190		2.31	8.45
	200		1.74	8.17
	210		1.00	7.81
	220		0.70	7.65
	230		0.39	7.46
	240		0.23	7.32
Started 30 sec irradn →	243			
	245			<0.5
Started 30 sec irradn →	247			
	249			~0

Table A- 3. Tabulated data for run EC-1769: O_3 + HBr with Irradiation

Initial O_3 = 17.8 ppm

	t (min)	O_3 Rel. Conc.	HBr (ppm)
Dark Decay →	0	1.0000	
	10	0.9950	
	20	0.9900	
	30	0.9656	
	41	0.9656	
	50	0.9513	
Added 20.0 ppm HBr →	56		
		(ppm)	
	59	15.25	16.54
	64	14.44	14.46
	69	13.94	13.28
	74	13.33	11.67
	79	12.43	9.99
Started Irradn →	81.5		
	83	~0	6.84
	88		6.19
	93		6.19
	98		6.16
	104		6.04
	109		5.98
	114		5.95
	119		5.80
Added 17.8 ppm O_3 → during irradn	122		
	124	~0	3.42
	130		3.42
	136		3.33

Table A- 4. Tabulated data for run EC-1770 : HBr + NO with Irradiation

Initial HBr = 20.0 ppm

	t (min)	HBr Rel. Conc.	NO (ppm)
Dark Decay →	0	1.0000	
	20	0.9950	
	30	0.9900	
	40	0.9802	
	50	0.9753	
	60	0.9705	
	70	0.9656	
	80	0.9608	
	90	0.9608	
	100	0.9561	
Added 10.0 ppm NO →	109		
		(ppm)	
	112	19.12	9.12
	122	19.12	8.89
	132	18.93	8.68
	154	18.74	8.29
	164	18.56	8.09
	174	18.37	7.89
	184	18.28	7.77
	194	18.19	7.62
Started Irradn →	198		
	200	18.10	7.77
	205	17.92	7.77
	210	17.83	7.77
	215	17.74	7.77
	220	17.48	7.70
	225	17.48	7.74
	230	17.31	7.70
	240	17.13	7.74
	250	16.96	7.74
	260	16.71	7.70
	270	16.55	7.66
	280	16.30	7.66
	290	16.06	7.70

Table A- 5. Tabulated data for run EC-1772 : HCHO + HBr + O_3 with Irradiation

	t (min)	HCHO (ppm)	HBr (ppm)	O_3 (ppm)	CO (ppm)
	0	7.04	20.00		
	10	7.04	20.00		
	20	7.04	19.90		
	30	7.01	19.90		
	40	7.01	19.70		
	50	6.97	19.65		
	60	6.97	19.60		
Added ~19 ppm O_3 →	64				
	67	6.90	17.57	17.80	0.05
	74	6.90	16.22	17.19	0.09
	79	6.87	14.90	16.52	0.12
	84	6.80	13.69	15.95	0.16
	89	6.80	12.02	15.17	0.19
	94	6.77	11.38	14.95	0.21
	99	6.73	10.25	14.50	0.22
	104	6.73	9.70	14.22	0.25
	109	6.73	8.78	13.73	0.27
	114	6.73	7.95	13.39	0.28
	119	6.73	7.48	13.19	0.29
Started 30 sec irradn →	122				
	123	5.22	7.71	10.02	1.85
Started 32 sec irradn →	126				
	127	4.09	7.56	7.85	2.78
Started 32 sec irradn →	130				
	131	2.68	7.30	5.16	4.25
Started 32 sec irradn →	134				
	135	1.60	6.45	2.81	5.16
Started 32 sec irradn →	138				
	139	0.52	5.72	0.71	6.04

Table A- 6. Tabulated data for run EC-1773: HBr + O_3 with Irradiation

	t (min)	HBr (ppm)	O_3 (ppm)	
Dark Decay →	0	10.00		
	10	9.95		
	20	9.90		
	30	9.83		
	40	9.71		
	50	9.66		
	60	9.61		
Added O_3 →	64			
(exact initial conc. not	67	8.03	18.34	
measured)	72	7.19	17.98	
	77	6.16	17.40	
	82	5.49	17.02	
	87	4.78	16.76	
	92	3.84	16.27	
	97	3.45	16.07	
	102	2.89	15.71	
	112	2.03	15.32	
	122	1.29	14.87	
	132	0.73	14.51	
	142	0.49	14.22	
	152	0.28	13.87	
	162		13.53	
Started 30 sec irradn →	167			
	168	-	6.76	
Started 30 sec irradn →	172			
	173	-	-	

Table A- 7. Tabulated data for run EC-1774: HBr + NO_2 with Irradiation

	t (ppm)	HBr (ppm)	NO_2 (ppm)	NO (ppm)
	0	20.00		
	10	19.80		
	20	19.41		
	30	19.41		
	40	19.22		
	50	19.22		
	60	19.22		
	70	19.03		
	80	18.93		
	90	18.74		
	100	18.56		
Added 10.4 ppm NO_2 →	118			
	122	18.37	10.38	
	132	18.83	10.38	
	142	18.74	10.38	
	152	18.56	10.38	
	162	18.37	10.38	
	172	18.19	10.38	
	182	18.01	10.38	
	192	17.83	10.38	
	202	17.65	10.38	
	212	17.48	10.38	
Started Irradn →	215			
	216	17.39	9.68	1.17
	226	17.22	8.63	2.30
	236	16.88	7.89	3.09
	246	16.63	6.79	3.72
	256	16.22	6.43	4.25
	266	15.90	5.94	4.75
	276	15.50	5.45	5.22
	286	15.27	5.11	5.54
	296	14.90	4.77	5.79
	306	14.60	4.38	6.06

Table A- 8. Tabulated data for run EC-1775: NO_2 + HCHO + HBr with Irradiation

	t (min)	HCHO (ppm)	NO_2 (ppm)	HBr (ppm)	CO (ppm)	NO (ppm)
Rxn mixture in the dark →	0	6.91	10.17	20.00		0.14
	10	6.84	10.17	19.90		
	20	6.87	10.12	19.70		
	30	6.84	10.02	19.51		0.26
	40	6.84	10.07	19.31		
	50	6.80	10.02	19.12		
	60	6.84	10.02	18.98	~0	0.43
Started Irradn →	63					
	66	6.34	9.35	18.93	0.45	0.75
	71	5.86	9.21	18.89	0.93	0.79
	76	5.35	8.76	18.84	1.42	0.90
	81	4.77	8.46	18.65	2.02	0.96
	86	4.39	8.25	18.65	2.47	1.03
	91	3.89	8.05	18.47	2.86	1.13
	101	3.08	7.81	18.28	3.53	1.30
	111	2.40	7.36	18.10	4.12	1.49
	121	1.78	7.07	17.92	4.58	1.73
	131	1.25	6.76	17.65	4.96	2.02
	141	0.46	6.43	17.31	5.21	2.35
	151	0.31	5.97	17.13	5.42	2.69
	161	0.20	5.65	16.80	5.56	3.05
	171	0.13	5.43	16.63	5.70	3.43
	181	0.07	4.82	16.30	5.76	3.78
	191	~0	4.65	16.06	5.78	4.11

Table A- 9. Tabulated data for run EC-1776: O_3 + HCHO + HBr with Irradiation

	t (min)	O_3 (ppm)	HCHO (ppm)	HBr (ppm)	CO (ppm)	CO_2 (ppm)
	0	18.12	7.08		0.05	0.18
Started Irradn →	11					
	14	16.98	6.44		0.68	0.22
	19	16.08	5.92		1.14	0.26
	24	15.30	5.35		1.72	0.31
	29	14.33	4.85		2.20	0.36
	34	13.37	4.34		2.63	0.42
	39	12.40	3.79		3.06	0.47
	44	11.34	3.28		3.46	0.51
Added 10.0 ppm HBr →	51					
	54	0.93	0.26	6.39	6.36	0.61
	57	-	-	4.76	6.53	0.64
	60	-	-	4.42	6.53	0.65
	63	-	-	4.31	6.53	0.66
	72	-	-	4.14	6.56	0.68
	81	-	-	4.02	6.56	0.70

Table A- 10. Tabulated data for run EC-1777: O_3 + HCHO + HBr with Irradiation

	t (min)	O_3 (ppm)	HCHO (ppm)	HBr (ppm)	CO (ppm)	CO_2 (ppm)
Dark period	0	18.66	6.10		0.06	0.10
	5	18.57	6.07		0.07	0.11
	10	18.57	6.07		0.08	0.11
	15	18.39	6.03		0.10	0.13
	20	18.29	5.98		0.12	0.14
	25	18.20	5.95		0.13	0.16
	30	18.20	5.92		0.14	0.16
	40	18.11	5.89		0.16	0.17
Started Irradn →	43					
	45	17.49	5.49		0.55	0.19
	50	16.64	5.04		0.96	0.23
	55	15.75	4.61		1.38	0.27
	60	14.91	4.17		1.84	0.31
	65	14.11	3.83		2.25	0.35
Added 9.98 ppm HBr →	69					
While being mixed	69.25	13.16	3.22	2.63	2.66	0.39
(mixing)	69.82	12.71	3.11	9.99	2.74	0.40
(mixing)	70.38	12.03	2.96	9.42	2.86	0.41
(mixing)	70.95	11.22	2.76	8.82	3.04	0.41
(mixing)	71.52	10.31	2.55	8.19	3.24	0.41
	73	7.57	1.87	7.67	4.07	0.42
	76	2.49	0.60	6.54	5.29	0.44
	79	0.18	0.03	4.30	5.82	0.48
	82	-	-	3.19	5.82	0.50

Table A- 11. Tabulated data for run EC-1778: O_3 + HBr with Irradiation.

	t (min)	O_3 (ppm)	HBr (ppm)	CO_2 (ppm)	HOBr (absorbance @ 1167 cm-1)
	-18	19.74			
	-5	19.60		0.05	
Added 10.0 ppm HBr →	0				
	4	18.93	8.70	0.08	-
	14	18.10	7.13	0.10	ca. 0.001
	24	17.48	5.75	0.12	ca. 0.001
	34	16.88	4.50	0.13	ca. 0.001
	44	16.30	3.10	0.16	ca. 0.0005
	54	15.82	2.25	0.18	-
	64	15.50	1.53	0.19	-
Started Irradiation →	66.5				
	67.5	2.86	1.11	0.21	
	69.1	-	0.96	0.21	
	72.0	-	0.68	0.22	

Table A- 12. Tabulated data for run EC-1779: NO_2 + HBr with Irradiation.

Initial NO_2 = 10.4 ppm
Initial HBr = 8.02 ppm (NO_2 first, then HBr at t = -6 min)

	t (min)	NO_2 (ppm)	HBr (ppm)	NO (ppm)	BrNO (ppm)	$BrNO_2$ (ppm)	HNO_3 (ppm)
	0	10.38	8.02		0.018		0.042
	10	10.35	7.90		0.028		0.037
	20	10.33	7.82		0.040		0.045
	30	10.28	7.74		0.049		0.047
	40	10.23	7.67		0.061		0.043
	50	10.12	7.52	0.23	0.070		0.045
	60	10.08	7.22	0.27	0.080		0.049
Started Irradn →	63						
	67	9.39	7.11	0.86	0.058	0.011	0.050
	72	8.84	7.01	1.40	0.070	0.006	0.062
	77	8.38	6.91	1.94	0.076	0.004	0.072
	82	7.93	6.81	2.37	0.082	<0.004	0.075
	87	7.54	6.74	2.76	0.085		0.076
	97	6.83	6.51	3.47	0.087		0.086
	107	6.30	6.32	3.99	0.087		0.084
	117	5.76	6.13	4.44	0.087		0.089
	127	5.40	5.95	4.80	0.084		0.089

Table A- 13. Tabulated data for run EC-1780: NO + HBr with Irradiation

	t (min)	NO (ppm)	NO_2 (ppm)	HBr (ppm)	BrNO (ppm)
	-9	9.67	0.33		
	-3	9.16	0.88		
Added 10.0 ppm HBr →	0				
	6	8.97	1.10	10.01	0.017
	18	8.71	1.34	9.76	0.050
	30	8.45	1.57	9.62	0.077
	37	8.33	1.71	9.52	0.086
	44	8.20	1.82	9.48	0.110
	51	8.08	1.94	9.38	0.120
	58	7.96	2.04	9.24	0.130
	65	7.84	2.15	9.20	0.150
	72	7.73	2.26	9.15	0.160
	79	7.61	2.34	9.10	0.170
	86	7.50	2.45	8.97	0.180
	93	7.42	2.54	8.92	0.190
	103	7.28	2.65	8.84	0.210
	113	7.17	2.76	8.66	0.230
	123	7.06	2.87	8.62	0.240
Started Irradn →	125				
	128	7.31	2.88	8.58	0.061
	133	7.31	2.89	8.53	0.058
	138	7.28	2.87	8.41	0.056
	143	7.31	2.87	8.36	0.056
	148	7.31	2.86	8.32	0.056
	158	7.28	2.85	8.20	0.057
	168	7.31	2.83	8.08	0.056
	178	7.24	2.81	8.00	0.056

Table A- 14. Tabulated data for run EC-1781: O_3 + HBr.

	t (min)	O_3 (ppm)	HBr (ppm)	HOBr (absorbance @ 1167 cm^{-1})
	-11	19.65		
	-6	16.65		
Added 4.00 ppm HBr →	0			
	4	19.11	3.49	-
	9	18.73	2.76	-
	19	18.27	1.98	-
	29	17.91	1.21	-
	39	17.82	0.94	-
	49	17.55	0.59	-
Added 4.00 ppm HBr →	54			
	57	17.16	3.88	-
	67	16.70	3.13	-
	77	16.29	2.50	-
	87	16.05	1.96	-
	97	15.77	1.27	-
Added 8.00 ppm HBr →	101			
	106	15.15	8.11	-
	116	14.34	6.45	~0.0005
	126	14.13	5.89	~0.0005
	136	13.44	4.43	-
	146	13.05	3.60	-
	156	12.66	2.75	-

Table A- 15. Tabulated data for run EC-1782: HCHO + O_3 + HBr with Irradiation

	t (min)	HCHO (ppm)	O_3 (ppm)	HBr (ppm)	CO (ppm)
	0	5.90	15.61		
	10	5.79	15.44		0.10
	20	5.76	15.36		0.14
	30	5.71	15.26		0.20
	40	5.65	15.14		0.23
Started Irradiation →	46				
Added 8.00 ppm HBr →	47				
	48	5.46	14.55	7.72	0.55
	50	4.91	13.17	6.99	1.13
	52	4.45	12.04	6.75	1.71
	54	4.05	11.11	6.52	2.15
	56	3.43	9.62	6.02	2.80
	59	2.66	7.53	5.26	3.64
	62	1.06	2.96	4.06	5.09
	65	0.18	0.48	3.63	5.79
	68	0.02	-	1.67	5.88
	71	-	-	1.04	5.88

Table A- 16. Tabulated data for run EC-1783: HCHO + Br_2 with Irradiation.

	t (min)	HCHO (ppm)	HBr (ppm)	CO (ppm)	HCOOH (ppm)	H_2O_2 (ppm)
	0	5.68				
	10	5.66				
	20	5.65				
	30	5.65				
Added 3.00 (?) ppm HBr →	40					
	43	5.63				
	53	5.61				
Started 15 sec irrdn →	60					
	62	4.27	1.43	1.58	0.06	0.34
Started 15 sec irrdn →	64					
	66	3.20	2.37	2.69	0.11	0.56
Started 15 sec irrdn →	69					
	71	2.16	3.13	3.74	0.14	0.76
Started 15 sec irrdn →	74					
	76	1.26	4.14	4.27	0.17	0.90
Started 15 sec irrdn →	79					
	81	0.62	4.69	4.84	0.18	0.95

Table A- 17. Tabulated data for run EC-1784: k_1 Measurement

N_2 diluent with <16 ppm O_2
Initial NO_2 conc.= 5.19 ppm

	t (min)	Rel. Conc.
	-3.50	1.0000
Started Irradn →	-1.00	
	0	0.8273
	1.067	0.7159
	2.133	0.6072
	3.200	0.4925
	4.250	0.4014
	5.300	0.3405
	6.367	0.2803
	7.433	0.2296

Table A- 18. Tabulated data for run EC-1785: HCHO + Br_2 with Irradiation.

	T (min)	HCHO (ppm)	HBr (ppm)	CO (ppm)	HCOOH (ppm)	H_2O_2 (ppm)
	0	6.00				
	6	5.98				
Added 3.00 ppm Br_2 →	12					
	15	5.97				
	20	5.97				
Started 15 sec irradn →	24					
	26	5.38	0.51	0.64	0.04	0.13
Started 15 sec irradn →	28					
	30	4.75	1.25	1.31	0.09	0.24
Started 15 sec irradn →	32					
	34	4.13	1.55	1.96	0.12	0.35
Started 15 sec irradn →	36					
	38	3.63	1.85	2.44	0.15	0.41
Started 15 sec irradn →	40					
	42	3.20	2.55	2.88	0.18	0.46
Started 15 sec irradn →	44					
	46	2.80	2.68	3.26	0.20	0.51
Started 30 sec irradn →	48					
	50	2.19	3.31	3.81	0.22	0.60
Started 30 sec irradn →	52					
	54	1.61	3.86	4.37	0.24	0.70
Started 30 sec irradn →	56					
	58	1.20	4.22	4.70	0.26	0.72

Table A- 19. Tabulated data for run EC-1786: NO_2 + Br_2 with Irradiation.

	t (min)	NO_2 (ppm)	NO (ppm)	$BrNO_2$ (ppm)	BrNO (ppm)
	0	5.19			
	12	5.19			
Injected 5.00 ppm Br_2 →	16				
	19	5.19			
	26	5.19			
Started 30 sec irradn →	31				
	33	5.08		0.029	0.020
Started 30 sec irradn →	35				
	37	5.04		0.028	0.021
Started 60 sec irradn →	39				
	41.5	5.01	0.11	0.025	0.026
Started 60 sec irradn →	44				
	46.5	4.98	0.17	0.023	0.030
Started continuous irradn →	49				
	51	4.77	0.35	0.039	0.008
	54	4.70	0.43	0.037	0.010
	57	4.63	0.51	0.036	0.011
	60	4.58	0.60	0.035	0.013
	63	4.51	0.66	0.034	0.014
	66	4.42	0.73	0.033	0.015
	69	4.35	0.82	0.031	0.016

Table A- 20. Tabulated data for run EC-1787: NO + Br_2 with Irradiation.

	t (min)	NO (ppm)	NO_2 (ppm)	$BrNO_2$ (ppm)	BrNO (ppm)	
	0	9.71	0.23			
	7	9.33	0.44			
Injected 5.00 ppm Br_2 →	14					
	17	9.28	0.72			
	22	9.15	0.85			
	27	9.05	0.98			
	33	8.92	1.12			
Started 30 sec irradn →	36					
	38	8.79	1.21		0.039	
Started 30 sec irradn →	40					
	42	8.66	1.3		0.042	
Started 30 sec irradn →	44					
	46	8.61	1.39		0.043	
Started 30 sec irradn →	48					
	50	8.53	1.48		0.044	
Started continuous irradn →	52					
	54	8.40	1.61	~0.006	0.040	
	57	8.44	1.66	"	0.041	
	60	8.36	1.72	"	0.042	
	63	8.28	1.76	"	0.042	
	66	8.24	1.81	"	0.043	
	69	8.20	1.86	"	0.043	
	72	8.15	1.91	"	0.044	
	77	8.07	1.98	"	0.045	
	82	7.99	2.05	"	0.046	
	87	7.91	2.11	"	0.046	

Table A- 21. Tabulated data for run EC-1788: Diethyl Ether + Br_2 with Irradiation.

	t (min)	Diethyl ether (ppm)	Ethyl formate (ppm)	HBr (ppm)
Initial Br_2 = 5.00 ppm	-5	5.00		
Started 60 sec irradn →	0			
	3	4.35	0.20	0.85
Started 60 sec irradn →	5			
	8	3.78	0.38	1.65
Started 60 sec irradn →	10			
	13	3.22	0.53	2.24
Started 60 sec irradn →	15			
	18	2.75	0.65	2.78
Started 60 sec irradn →	20			
	24	2.30	0.78	3.42
Started 60 sec irradn →	26			
	29	1.97	0.87	3.82
Started 60 sec irradn →	31			
	34	1.64	0.97	4.42
Started 60 sec irradn →	36			
	39	1.36	1.05	4.78
Started 60 sec irradn →	41			
	44	1.11	1.13	5.21

Table A- 22. Tabulated data for run EC-1789: p-Xylene + 1,3,5-Trimethylbenzene + Br_2 with Irradiation.

	t (min)	p-Xylene (ppm)	1,3,5-TMB (ppm)	HBr (ppm)
Initial Br_2 = 10.0 ppm	-3	5.00	2.58	0.00
Started 60 sec irrad'n →	0			
	3	3.97	1.87	3.10
Started 60 sec irrad'n →	6			
	9	3.47	1.54	3.96
Started 60 sec irrad'n →	12			
	15	2.64	1.04	6.08
Started 60 sec irrad'n →	18			
	21	2.34	0.84	6.33
Started 60 sec irrad'n →	24			
	27	1.82	0.62	7.35
Started 60 sec irrad'n →	30			
	33	1.55	0.49	7.57

Table A- 23. Tabulated data for run EC-1790: HBr + HNO_3.

	t (min)	HBr Rel. Conc.	HNO_3 Rel. Conc.
Injected 20.0 ppm HBr →	-3		
	0	1.0000	
	10	0.9851	
	20	0.9753	
	30	0.9753	
	40	0.9656	
	50	0.9561	
	60	0.9466	
Added ~10 ppm HNO_3 →	67		
	71	1.0000	1.0000
	76	0.9950	0.9681
	81	0.9950	0.9466
	86	0.9900	0.9250
	91	0.9900	0.9141
	96	0.9850	0.8984
	101	0.9851	0.8851
	106	0.9802	0.8740
	116	0.9802	0.8500
	126	0.9802	0.8300
	136	0.9753	0.8110

Table A- 24. Tabulated data for run EC-1791: Cyclohexane + 2,3-Dimethylbutane + Br_2 with Irradiation.

	t (min)	Cyclohexane (ppm)	2,3-Dimethyl-butane (ppm)
Initial Br_2 = 10.0 ppm	0	5.00	5.00
After two 60 sec periods of irradn →	13	5.00	4.95
After two 60 sec periods of irradn →	23	5.00	4.88
After two 60 sec periods of irradn →	33	5.00	4.83
Started continuous irradn →	36		
	40	5.00	4.76
	46	5.00	4.69
	52	4.98	4.55
	58	4.95	4.41
	64	4.95	4.33

Table A- 25. Tabulated data for run EC-1792: O_3 + HBr with Irradiation.

Note: 300 ppb of cyclohexane was added as OH tracer, but its analysis by GC for this run was erratic.

	t (min)	O_3 (ppm)	HBr (ppm)
	0	20.04	
	5	19.94	
	10	19.84	
	15	19.74	
	20	19.62	
	25	19.50	
	30	19.38	
	35	19.30	
	40	19.25	
	45	19.16	
	50	19.12	
	55	19.22	
	60	19.16	
	79	18.97	
	100	18.78	
Added 20.0 ppm HBr →	107		
	111	18.05	17.65
	118	17.51	16.38
	125	16.75	15.05
	132	16.17	13.62
	139	15.31	11.90
	146	14.86	10.99
Started irradn →	149		
	151	0.35	7.67
	156	-	6.71
	161	-	6.48
	166	-	6.35
	171	-	6.32
Stopped irradn →	173		
	175	-	6.32
Added O_3 →	178		
	181	19.94	5.80
Started irradn →	184		
	186	0.10	3.89
	191	-	3.05
	196	-	3.03
	201	-	2.99
	206	-	2.89

Table A- 26. Tabulated data for run EC-1793: k_1 Measurement.

N_2 diluent with <2.8 ppm O_2
Initial NO_2 conc.= 5.19 ppm

	t (min)	NO_2 Rel.Conc.
	-4.783	1.0000
Started Irradiation →	-1.000	
	0	0.8069
	1.067	0.6609
	2.133	0.5551
	3.200	0.4755
	4.267	0.3895
	5.333	0.3159
	6.400	0.2680
	7.467	0.2273

Table A- 27. Tabulated data for run EC-1795: HCHO + NO_2 + Br_2 + n-Heptane tracer, with Irradiation

	t (min)	HCHO (ppm)	NO_2 (ppm)	n-Heptane (ppm)	HBr (ppm)	CO (ppm)	CO_2 (ppm)	HCOOH (ppm)
Injected HCHO →	0	5.76						
	8	5.73						
Added n-Heptane and NO_2 →	~20							
(n-Heptane analysis by GC)	25	5.73	5.19	0.30				
Added Br_2 (3.00 ppm) →	~34							
	38	5.73	5.19	0.30				
	68	5.67	5.16					
	92	5.62	5.16					
Started 30 sec irradn →	95							
	99	5.06	4.58	0.29	-	0.62	0.013	0.016
	123	5.06	4.60		-	0.59	0.017	0.017
	134	5.03	4.63		-	0.59	0.019	0.018
Started 60 sec irrad →	139							
	142	4.08	3.66	0.29	0.87	1.61	0.025	0.039
	164	4.04	3.62		-	1.61	0.035	0.039
Started 90 sec irradn →	168							
	172	2.71	2.43	0.29	1.03	3.11	0.045	0.065
	185	2.70	2.48		-	3.11	0.054	0.073
Started 90 sec irradn →	196							
	201	1.45	1.69	0.29	1.10	4.49	0.068	0.085
	211	1.45	1.91		-	4.49	0.081	0.090

Continued on next page

Table A- 27 (continued)

	t (min)	N_2O_5 (ppm)	HONO (ppm)	$HOONO_2$ (ppm)	$BrNO_2$ (ppm)	BrNO (ppm)
Injected HCHO →	0					
	8					
Added n-Heptane and NO_2 →	~20					
(n-Heptane analysis by GC)	25					
Added Br_2 (3.00 ppm) →	~34					
	38					
	68					
	92					
Started 30 sec irradn →	95					
	99	0.08	0.05	0.27	0.019	-
	123	0.04	0.10	0.10	0.003	0.007
	134	0.02	0.11	0.07	0.003	0.009
Started 60 sec irrad →	139					
	142	0.13	0.15	0.59	0.021	-
	164	0.12	0.21	0.28	0.003	-
Started 90 sec irradn →	168					
	172	0.23	0.24	0.88	0.015	0.004
	185	0.23	0.27	0.54	0.007	0.015
Started 90 sec irradn →	196					
	201	0.26	0.28	0.97	0.011	0.003
	211	0.22	0.28	0.55	0.005	0.012

Table A- 28. Tabulated data for run EC-1796: O_3 + HBr +Cyclohexane tracer, with Irradiation

All analysis by FTIR

	t (min)	O_3 (ppm)	HBr (ppm)	Cyclohexane (ppm)
	0	20.02		0.40
	5	20.02		0.40
	15	20.02		0.40
	25	19.92		0.40
	35	19.92		0.40
	45	19.82		0.40
Added 20.0 ppm HBr →	49			
	53	19.33	18.01	0.40
	58	18.67	16.88	0.40
	68	17.67	14.75	0.40
	78	16.73	12.89	0.40
	88	15.99	11.38	0.40
	98	15.29	10.10	0.40
	108	14.77	8.74	0.40
	118	14.26	7.71	0.40
Started Irradn →	121			
	123	0.44	5.55	0.37
	128	-	5.25	0.36
	133	-	5.02	0.34
	138	-	4.85	0.34
	143	-	4.85	0.34
Added 20.0 ppm O_3 while irradiating →	146			
	148	-	3.02	0.33
	153	-	3.00	0.32
	158	-	3.00	0.32
	163	-	3.00	0.32

Table A- 29. Tabulated data for run EC-1797: O3 + HCHO + HBr + Cyclohexane tracer, with Irradiation

	t (min)	O3 (ppm)	HCHO (ppm)	HBr (ppm)	Cyclohexane (ppm)	CO (ppm)
	0	20.11			0.40	
	10	20.01			0.40	
Added 7.09 ppm (calc'd) HCHO →	16					
	20	19.81	7.08		0.40	-
	30	19.71	7.01		0.40	0.05
	40	19.61	6.94		0.40	0.08
	50	19.52	6.87		0.40	0.10
Started Irradn →	52					
	54	19.23	6.67		0.39	0.28
	60	18.75	6.44		0.37	0.68
	66	18.20	6.13		0.36	1.06
	72	17.58	5.66		0.35	1.47
	78	16.89	5.20		0.34	1.87
	84	16.15	4.75		0.33	2.29
	90	15.44	4.34		0.32	2.66
	96	14.69	3.91		0.31	3.01
Added 10.0 ppm (calc'd) HBr while irradiating →	99					
	102	10.36	2.73	7.67	0.30	4.44
	105	4.12	1.04	6.47	0.30	5.93
	108	-	-	4.78	0.28	6.79
	111	-	-	3.54	0.26	6.79
	114	-	-	3.25	0.26	6.80
	117	-	-	3.16	0.26	6.80

Table A- 30. Tabulated data for run EC-1798: HBr + O_3 in Diluent Air with added H_2O (25% RH)

	t (min)	HBr (ppm)	O_3 (ppm)
Injected 20.0 ppm (calc'd) HBr →	-3		
	0	15.90	
	5	14.98	
	10	13.69	
	15	12.77	
	20	12.21	
	25	11.33	
	30	10.51	
	35	10.20	
	40	9.37	
Injected ~20 ppm O_3 →	43		
	45	6.48	19.05
	50	5.36	18.49
	55	4.50	18.21
	60	2.96	17.76
	65	2.38	17.41
	70	1.90	17.24

Table A- 31. Tabulated data for run EC-1799: HBr + O_3 in Diluent Air with added H_2O (13% RH).

	t (min)	HBr (ppm)	O_3 (ppm)
Injected 20.0 ppm (calc'd) HBr →	-3		
	0	18.48	
	5	17.93	
	10	17.58	
	15	17.15	
	20	16.81	
	25	16.48	
	30	16.31	
	35	16.15	
	40	15.91	
	45	15.67	
	50	15.52	
	55	15.29	
	60	15.06	
Injected ~20 ppm O3 →	66		
	70	13.23	19.65
	75	11.91	18.51
	80	10.73	18.05
	85	9.91	17.52
	90	8.70	16.92
	95	8.07	16.67
	100	7.13	16.18
	105	6.20	15.94
	110	5.72	15.54
	115	5.13	15.24
	120	4.53	14.86
	125	4.20	14.42
	130	3.88	14.00